University of Groningen

July 5, 2019

Bachelor Thesis

Negative Leader Propagation

Author
B. Neijzen
S3008681

Supervisor
O. Scholten
Second Examinor
J. G. Messchendorp

Abstract

This research focuses on the propagation of negative lightning leaders. According to current understanding, the negative leaders propagate step-wise. Measurements from LOFAR are used to analyze leader propagation in more detail. This data indeed shows temporal stepping behaviour. However, it shows Bursts of Very High Frequency (VHF) radiation for every step instead of a single pulse. Besides, the spatial propagation of the negative leader does not exhibit a clear stepping behaviour. Due to the bursts being more spread out in space, they overlap with each other, making the propagation seem more continuous. An average stepping length can be measured, however. The found values are

- Stepping time: $40 - 100$ μs
- Stepping length: $5 - 10$ m
- Spatial separation inside a burst: $2 - 10$ m
- Temporal separation inside a burst: $1 - 10$ μs

Two models concerning the emission of VHF are discussed. Firstly, the electromagnetic emission from an accelerated point charge is modelled. However, the power output from this model does not reproduce the measured values. Measurements show peaks that are much lower than are predicted by this model. Secondly, streamer collisions and propagation are scrutinized. VHF emission by streamers does not reproduce the measurements very well since it predicts VHF radiation over elongated periods. Where the data shows radiation spread over a mere $1 - 10$ μs. Hence, more research has to be done into the mechanism that is responsible for the emission of VHF radiation in negative leaders.

Contents

1 Introduction

Lightning, despite being familiar to humans since the start of our existence, is still a very poorly understood field in physics today. Our understanding of lightning breaks down at even the simplest of questions, like *How does lightning start?*, *How does it propagate?* or *How does it connect to ground?* [1]. This research will not address all these questions, but will look at some finer details of a lighting flash.

A lightning flash has two different stages. First, the flash has to be initiated. This initiation involves the emergence of a dipole. Both ends of this dipole can grow up to lengths of multiple kilometers and are referred to as leaders. The way these opposite charged leaders propagate however, is completely different. The mechanism behind lightning initiation and leader propagation is explained in section 2. As it turns out, lightning leaders emit Very High Frequency (VHF) radiation during their propagation. The Low-Frequency ARray(LOFAR) is capable of measuring this radiation and thus allows deeper research into the physics behind the propagation of lightning leaders. The main research of this paper is about the propagation of the negative leader. It is expected to propagate step-wise, which would show VHF emission in regular intervals [2]. This assumption will be checked with the LOFAR measurements. In addition to this, other features of the negative leaders will be scrutinized. This is done to make clear physical distinctions between the different types of leaders. Features that will be scrutinized are:

- What is the stepping time between these VHF emissions?
- How does the negative leader propagate in space?
- Is there a correlation between stepping time and location in space?

By looking into these features, a clear picture can be made of how a negative leader should look. Ideally, the negative leaders would be distinguished by an algorithm. Currently, this is not possible, since the features of the negative leaders are not known well enough to write an algorithm which detects the negative leaders with high enough precision. This is where this research is important. By analyzing the features and making clear what distinguishes a negative leader, it could be made possible to automatize the detection of these leaders. By automatizing this detection, time and human resources are saved, as well as the fact that subjectivity of the observer is taken out of the process.
Besides, this research will look into possible sources of VHF radiation. Even though detecting this VHF emission gives insight into how lightning works, it is still unknown what the source is of this VHF radiation. Models of sources will be critically analyzed with the obtained data to check whether they hold up.

2 Theory

In this section, the theoretical background of lightning will be discussed. The main focus will lie on the initiation of lightning, as well as the propagation mechanisms of the positive and negative leaders.

2.1 The Initiation of Lightning

The initiation of lightning is built up of two parts. At first, the separation of charges in the cloud has to occur. Secondly, the lightning flash has to start propagating. The precipitation model is a model that attempts to explain how charges are separated and is described below.

Precipitation Model

In the precipitation model, it is theorized that the separation of charge in the thundercloud is initiated by the collisions of ice crystals, raindrops and graupel in the cloud. Strong convective air currents blow up through the cloud. The heavier and larger particles are pulled downward by gravity, which balances the force of the air flows. The smaller raindrops are not pulled down as much and are blown up by the air flow. When these lighter particles are blown up, they travel through a mist of more massive particles which can cause collisions. During these collisions, charges can be transferred. This is comparable to rubbing hands over a balloon. While rubbing, charges are transferred from the hand to the balloon making one of the two positively charged and the other negatively charged. The collisions of the ice particles are no different. They are "rubbed" together, and during this process they transfer charges. The sign of charge the more massive particles pick up depends on the temperature. Above a certain temperature, referred to as T_R, it is more likely for the heavier particles to pick up a positive charge. If the temperature is below T_R, they are more likely to pick up a negative charge. Due to charge conservation, the smaller ice particles will get charged by the same amount but with opposite sign, which creates charge separation inside the thundercloud. Since the bottom of the cloud now has a charge, it will repel the opposite sign charges on the ground. Consequently, the ground will get charged by induction [3]. This can be visualized by use of figure 2.1.

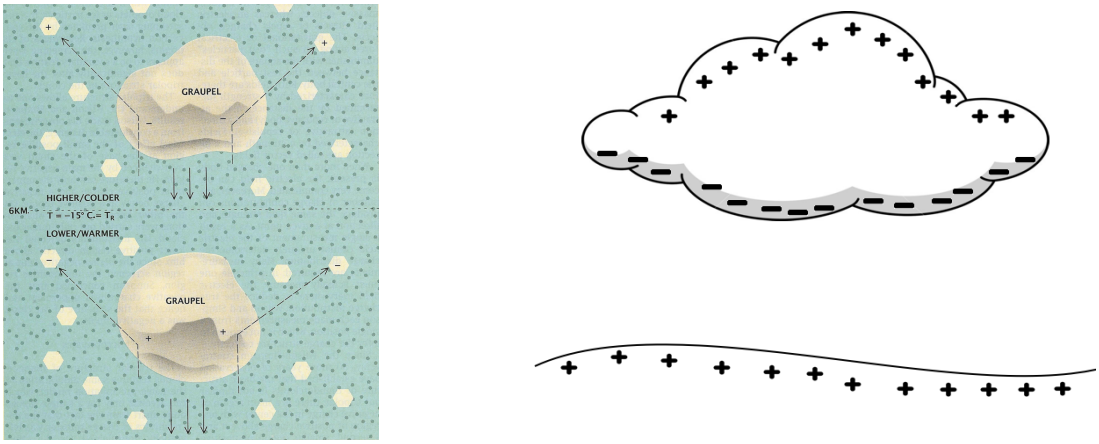

(a) (b)

Figure 2.1: (a) Shows the collisions of the ice crystals that cause the charge separation [3]. (b) Shows the charge separation in the cloud after the collisions. In this case a positive dipole structure.

Initiation of Lighting in a Thundercloud

The second part of lightning initiation is the actual start of a leader channel*. Initiation of the leader channel remains one of the biggest unanswered question in lightning physics to date. It is assumed to start by the heating of air due to streamers. In weaker electric fields, streamers are weak and propagate at relatively low speeds. After these streamers propagate for a short distance, they become electrically isolated from their point of origin. This means, once the streamer becomes isolated, it can no longer heat up the air at the point of origin. In stronger electric fields, streamers propagate faster and are able to collect more charge at their tip. Also, they do not become electrically isolated as fast and are able to create longer channels. Streamers in this stronger electric field, can also branch, allowing multiple streamer channels to collect charge and supply it back to the initial streamer channel. This process heats up the surrounding air and can initiate a leader. The exact electric field strength necessary for this to occur is unknown, but seems to be much higher than the field strengths measured in thunderclouds. Hence, something about our understanding is wrong, or unknown processes allow small regions inside the thundercloud to create an increased electric field.

2.2 Propagation of Positive Leaders

Positive Leaders are characterized by their continuous propagation. The tip of the positive leader is positively charged. At the tip of the leader, smaller structures, called streamers, are formed which propagate out in front of it. Positive streamers have a positively charged head. The positive charge on the head of the streamer attracts free electrons in the surrounding area. In the atmosphere, free electrons are mainly generated by two phenomena, natural

*Leaders and streamers will be discussed in more detail in section 2.2 and 2.3.

radioactivity and cosmic radiation. These free electrons attach to oxygen, which becomes negatively charged. Since these oxygen atoms are now negatively charged, they are attracted to the positive streamer head and thus drift towards it. This creates an ionized region of air around the leader called the corona. During this process, they can collide with other atoms in the atmosphere which can create new free electrons. These free electrons are then accelerated towards the positive streamer. The accelerated electron can create an avalanche. An avalanche is a reaction in which the electron collides with atoms which consequently produces more free electrons. If this happens in an area where ionization probability is higher than attachment probability, it creates a chain reaction. This chain reaction consists of the first electron colliding with an atom, creating new free electrons. Then the new free electrons collide with other atoms to create even more free electrons and so forth [4]. The electron avalanche moving towards the positive streamer creates a net positive charge. The propagation of the positive streamer then consists of a series of electron avalanches. These streamers carve out the path for the positive leader which propagates behind the streamers. [2].

2.3 Propagation of Negative Leaders

The negative leader propagates in a different fashion than the positive leader. First of all, it does not propagate continuously, but in a step-wise manner. Meaning it makes sudden jumps in space after standing still for a short time. Negative streamers do not help the propagation of negative leaders in the same way. Negative streamers propagate less easily since the volume of air around the negative streamer that contains electrons which can form avalanches, is much smaller than that of a positive streamer. This step-wise propagation can also be explained by means of electron avalanches. Again free electrons can be generated by natural radioactivity and cosmic radiation. These attach to oxygen to create negative ions. Since the leader, in this case, is negatively charged, the oxygen ions drift away from the leader. The process is the same as for the positive leader, but now electron avalanches are created a distance away from the leader. Here a so-called space stem is created. This is a warmer segment where the temperature is high enough to emit visible light. It starts to propagate bidirectionally until it connects back to the negative leader. When this happens, the negative leader jumps and increases in length suddenly. This is one step in the propagation. The propagation of a negative leader consists of a repetition of this process.

The emergence of this space stem is a topic which is currently not well understood. However, a recent study did shed some light on the mechanisms behind it [5]. The simulation done in this study does involve leader propagation in laboratory conditions. However, since laboratory sparks and lighting share a lot of common features, it is accurate to say that lightning behaves the same. In this simulation, it is found that the space stem is not formed by random disturbances in the conductivity or density of the gas surrounding the leader. Instead, the space stem is formed by a narrowing of the streamer channel. In figure 2.2 such a narrowing is visualized. Near the leader, the streamer head is wide. This occurs due to the curvature of the leader tip, which makes the electric field in that location non-uniform. Further away from the leader tip, the electric field becomes more homogeneous and this causes the streamer head to narrow. The narrowing causes higher electric fields and the conductance per unit length reaches a minimum. This creates a locally bright and warmer region, which consequently evolves into a space stem.

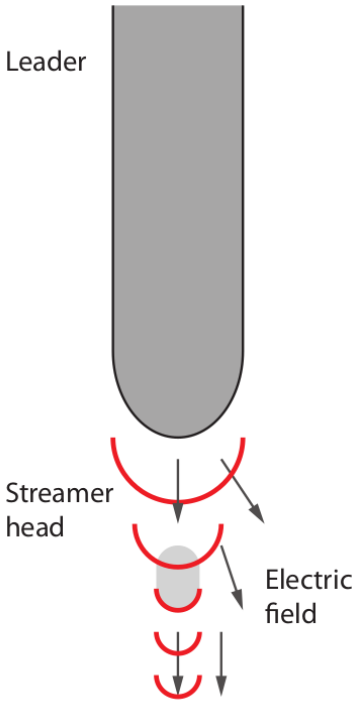

Figure 2.2: Narrowing of the streamer channel farther away from the tip of the negative leader [5].

3 Detection of lightning leaders

The detection of the propagation of lightning leaders is a difficult topic. They travel at high speeds and are often kept out of view by the cloud in which they are formed. Optical detection methods are thus out of the question. This is where LOFAR comes in. As it turns out, lightning leaders emit VHF radiation during their propagation. This radiation has a frequency of about 60MHz. LOFAR is capable of operating in this frequency range and can thus play a crucial role in detecting the propagation.

3.1 LOFAR

LOFAR is a radio interferometer located in the north-eastern part of the Netherlands, initially intended for the low-frequency band of astrophysical studies. However, it turned out to be a useful tool for the imaging of lightning flashes. LOFAR consists of 48 stations with low cost and small receiving elements. These stations are located in the Netherlands as well as in Germany, France, UK and Sweden. 40 Of these stations are placed in the North-Eastern part of the Netherlands and cover an area of 180 km in diameter. A single antenna performs very basic functions, but the fact that there are a lot of antennas distributed over such a large area makes it useful for multiple scientific studies. These antennas provide collecting area, raw sensitivity and pointing and tracking capabilities. The pointing and tracking mechanism works by combining signals from multiple antennas to deduce the location of the source. LOFAR is capable of operating in the 10-240 MHz range. This is achieved by the use of two different antennas, the low band antennas(LBA's) and high band antennas(HBA's). The LBA's operate at $10-90$ MHz. The lower part of this spectrum is dominated by strong radio frequency interference (RFI), and the high part of the spectrum lies close to the FM band. Hence, a filter is used to block the noisy parts of the spectrum, which limits the spectrum to 30-80 MHz. Also, LBA's can monitor the whole sky and can be used to create a sky map at the scale of seconds. The HBA's cover the higher part of the spectrum, namely 110-250 MHz, but these antennas are focused on a narrower part of the sky and can thus not create a sky map. Since lightning leaders emit radiation in the 60 MHz region and travel at high speed over large distances, the pointing and tracking capabilities as well as the frequency spectrum of the LBA's make for a clear choice of which antenna should be used for the imaging of lightning [6].

3.2 Data Processing

After obtaining the raw data, it has to be processed. In this section, the main features of the processing pipeline will be explained. The pipeline is shown schematically in the figure below.

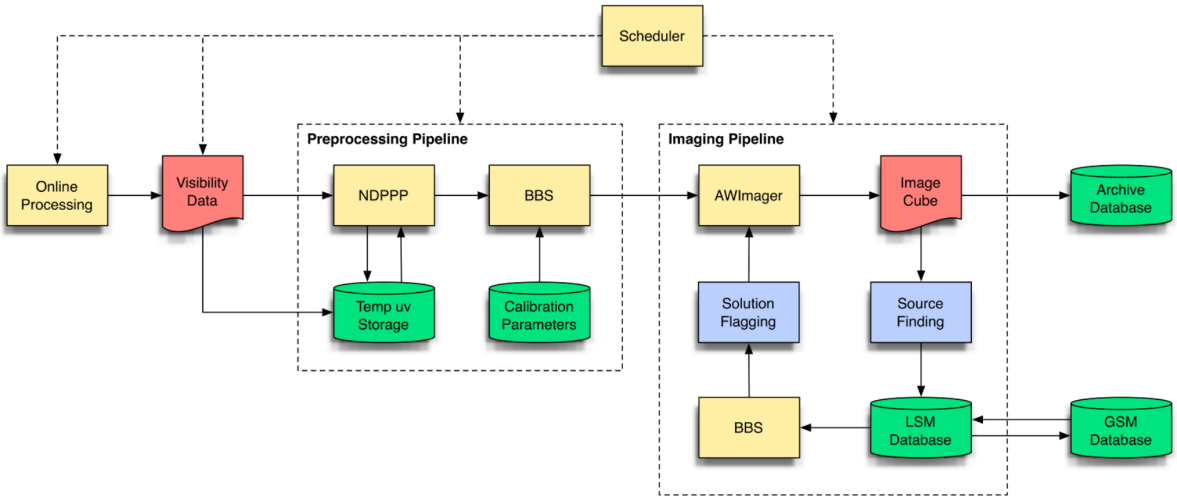

Figure 3.1: Schematic pipeline of data processing at LOFAR [].

The data processing starts with the visibility data running through the NDPPP. NDPPP stands for New-Default Pre-Processing pipeline, this pre-processing software flags the data in time and frequency. In addition to this, there is an option to average it over time, frequency or both. NDPPP also includes subtraction of the brightest sources in the sky. After this is done, an initial set of calibration parameters is applied. The calibration used initially comes from observations made of the background. This observation can be made parallel to or just before the actual measurement. Then the BBS is applied, which stands for blackboard selfcal and is a phase calibration. The phase calibration makes use of the local sky model (LSM), which is generated from the global sky model (GSM). The GSM comes from sky surveys of multiple sources [7, 8, 9]. Following the phase calibration, a w- and A-projection algorithm is applied. LOFAR has a large sky coverage and is thus subject to distortion of sources due to beam effects facet imaging can be used to account for non-co-planar baselines and the w-projection algorithm helps with this. It makes sure the maximum facet size is not restricted by the effect non-co-planar baselines [10]. The A-projection algorithm can correct for any directional dependent effects [11]. In the next step, source finding software is used to identify detected sources. Subsequently, an updated LSM is generated. This process of finding sources and updating the LSM is repeated multiple times. In the end, the final LSM is used to update the GSM, which produces the final image [6].

4 Models

As discussed before, a lot about lightning is unknown, but there are models that attempt at explaining the phenomena observed. Here two models for the emission of VHF radiation will be discussed. Later the obtained data is compared to what is expected from the models.

4.1 Accelerating Charge

The first model deals with the radiation emitted by an accelerated point charge. A negative leader propagates step-wise, which means the charge in the leader channel does so too. Hence, it accelerates twice every step. This model is simplified and only attempts to give an order of magnitude estimation of what would be measured due to this acceleration.

As stated before, a negative leader propagates step-wise. This could be simplified to a certain amount of charge propagating step-wise. In this stepping process, the charge first stands still, then suddenly starts moving at a very high speed and subsequently decelerates rapidly until it is stationary again. This could be visualized by the use of figure 4.1. Here a charge Q is stationary at $t < t_1$, suddenly moving at $t_1 < t < t_2$ and stationary again at $t > t_2$. In this time it has moved a distance x. Assuming the speed of the moving charge is very high, a value close to the speed of light can be taken. In this case $\frac{c}{3}$ is used. Given these values, the current during the step can be determined.

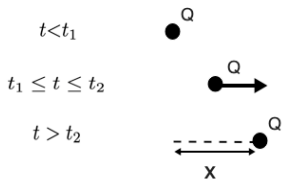

Figure 4.1: Step-wise moving point charge.

$$I = \frac{q}{t} = \frac{Q \cdot v}{x} = \frac{Q \cdot c}{3x} \ .$$

The current is only non zero during the step, but zero before and after. This results in the following current

$$I = \begin{cases} 0, & \text{if } t < t_1 \\ \frac{Q \cdot c}{3x}, & \text{if } t_1 < t < t_2 \\ 0, & \text{if } t > t_2 \ . \end{cases}$$

Another assumption in this model is that the charges have such high acceleration that it takes barely any time to reach their maximum speed, and thus the maximum current. The change in current is the important property since the electric field emitted is proportional to the change in current. The change in current can be most easily visualized in figure 4.2.

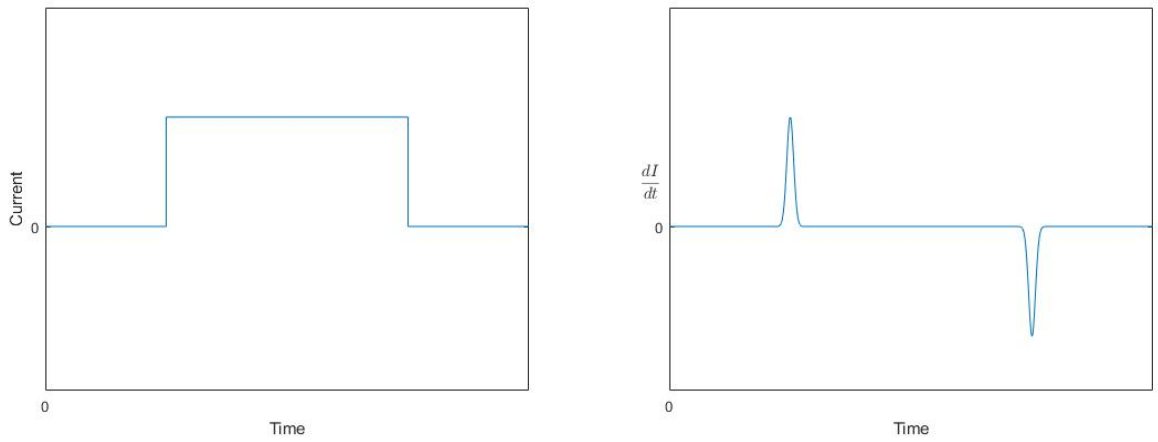

(a) (b)

Figure 4.2: (a) Shows the current versus time, showing the rapid acceleration and deceleration. (b) Here the change in current is shown. Two spikes according to the rapid increase and decrease of the current.

A change in current creates electromagnetic radiation. As can be seen from the graph, the change in current is only non-zero at $t = t_1$ and $t = t_2$. Mathematically this looks like

$$\frac{dI}{dt} = \delta(t - t_1)\frac{Q \cdot c}{3x} - \delta(t - t_2)\frac{Q \cdot c}{3x} \ .$$

Since the change in current is only non-zero at times t_1 and t_2, the electromagnetic radiation is also only non-zero at these times. Expressing the electric field as

$$E = -\nabla\phi - \frac{d\mathbf{A}}{dt} \ ,$$

where ϕ is the electric potential. Assuming ϕ is constant during the step taken by the point charge, its derivative drops out. Using the vector potential, given below, the electric field can be deduced,

$$A^\mu = \frac{1}{4\pi\epsilon_0 c^2}\int dx^3 \ \frac{j^\mu}{D} \ ,$$

where D is the distance from the charge to the antenna and $\frac{1}{4\pi\epsilon_0 c^2}$ ensures the units are correct. Taking the derivative and equating it to the electric field gives the desired result.

$$E = -\nabla\phi - \frac{d\mathbf{A}}{dt} = \frac{1}{4\pi\epsilon_0 c^2}\int dx^3 \ \frac{\frac{dj^\mu}{dt}}{D} \ .$$

Now to work out the expression for the electric field, the integral, as well as the value for $\frac{dI}{dt}$, should be computed. The integral can be simplified by assuming the negative leader is a straight line. This approximation is valid since a negative leader can easily be much longer than it is wide. An integral over a straight line gives back the length of the line along which the charge travels. Since it is approximated to be a point charge, all the charge is confined

in the tip of the leader, and the length along which the charge travels is only the length of the step, x.

$$E = \frac{1}{4\pi\epsilon_0 c^2}\frac{x}{D}\frac{dj^\mu}{dt} \ . \tag{4.1}$$

Turning to the value of $\frac{dI}{dt}$, a problem occurs. As can be seen in figure 4.2b, the change in current is characterized by two delta spikes. Simply taking the values of $\frac{dI}{dt}$ at $t = t_1,\ t_2$ gives infinity. Instead of ramping the current up infinitely fast, which results in the delta spikes, the current is approximated to increased steadily during a certain time, τ. The resulting change in current is not a delta spike, but two step functions. If the current is increased at a constant rate during a time τ, the resulting change in current is $\frac{dI}{dt} = \frac{Q\cdot c}{3x\cdot\tau}$. The expression for the electric field then becomes

$$E = \begin{cases} \frac{1}{4\pi\epsilon_0 c^2}\frac{Q\cdot c}{3D\cdot\tau} & \text{if } t_1 < t < t_1 + \tau \text{ and } t_2 < t < t_2 + \tau \\ 0 & \text{otherwise.} \end{cases}$$

From the electric field, the power density can be determined. This is the amount of energy reaching the antenna location per meter squared. This is given by the following expression.

$$P_D = \frac{E^2}{Z_0} = \frac{(\frac{1}{4\pi\epsilon_0 c^2}\frac{Q\cdot c}{3D\cdot\tau})^2}{Z_0} \ , \quad \text{where } Z_0 = \frac{1}{\mu_0 c} \ .$$

This power density is what LOFAR can possibly measure and could be visible in the data. A charge of 3 mC is a realistic amount for the tip of a negative leader [12]. Taking the following values:

- Q=3 mC
- D=7 km
- Z_0= 377 Ω
- τ=1 ns

yields a power density of $P_D \approx 4.8{\cdot}10^4 \frac{\mathrm{W}}{\mathrm{m}^2}$*. The collecting area of an antenna is approximately 1 m^2, so the power power measured is $P \approx 4.8 \cdot 10^4$ W

Now two questions arise: *How can it be certain that this is measured by the LOFAR antennas?* and *how would this look like in the data if it were to be measured?*
The first question can be answered by looking at two different things. Firstly, the pulse should lie in the frequency range in which LOFAR operates, and secondly, the pulse should create significantly higher power at the antenna then the background for it to be visible. The latter is a simple comparison between the power calculated and the background. The background can be seen in figure 4.3.

*The reason these values are taken will become clear in the results section.

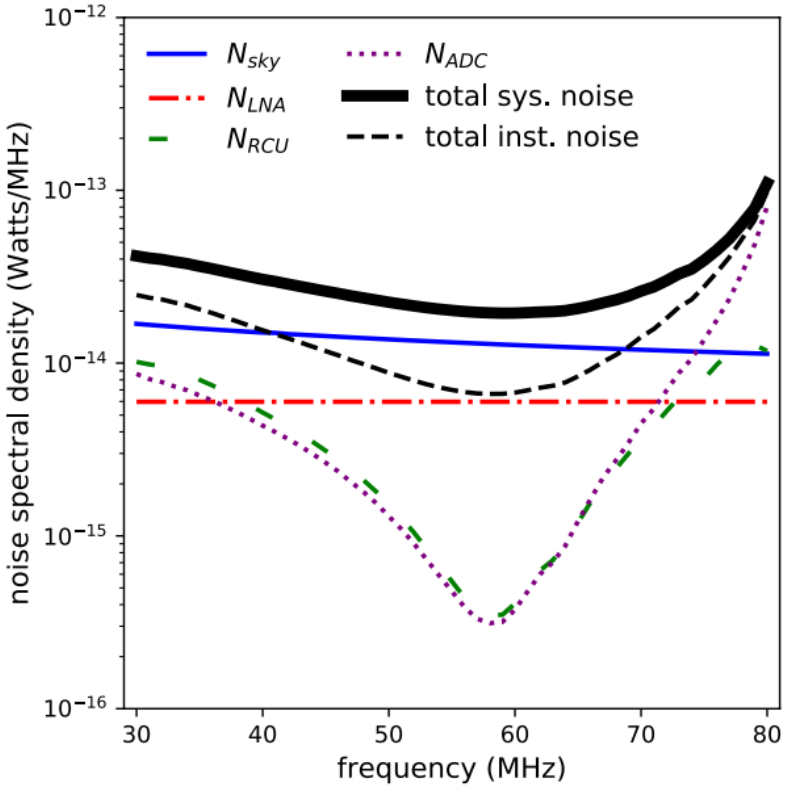

Figure 4.3: A graph showing the background noise for the frequency region used for lightning measurements by LOFAR. The total system noise contains the noise from all sources, i.e. sky and instrumental noise [13].

Note that the noise at all frequencies in this range is of the order of $10^{-13}\frac{\text{W}}{\text{MHz}}$ or less. As can be seen from the calculation above, the power due to the moving charge is of the order of 10^4 W. Granted, since the graph is in $\frac{\text{W}}{\text{MHz}}$ it should be integrated, the integration window is 50 MHz so this brings the order of magnitude to 10^{-12}. Also, at larger angles, the LBA antennas are less sensitive. Since lightning moves over large distances it is fair to assume a lot of the measurements happen at large zenith angles from the LBA antenna, further reducing the difference between background noise and signal. This lowering sensitivity could decrease the signal by a factor of 100 [14]. Then the signal is of the order of 10^2 W. However, the difference in order of magnitude between signal and background is still 10^{14}, thus, the pulse would reach far above the background noise. Hence, if it has the right frequency, it would be visible for LOFAR.
Now the second part of the question is whether the pulse is in the frequency range in which LOFAR operates. To check this, the frequency of the emitted radio waves should be determined. The wavelength of emitted waves can be deduced from the step length. The step taken by the charge is of the order of half a wavelength. In the model used, the step length, x, is 10 m, so then the wavelength, λ, is 20 m. From this, the frequency of the wave

with maximum power can be determined by the simple equation

$$\nu = \frac{v}{\lambda} = \frac{c}{3\lambda} = \frac{c}{3(2x)} = 5\,\text{MHz}\ .$$

Lightning measurements of LOFAR operate in the $30 - 80$ MHz region, meaning this does fall below it. However, a pulse emits in a range around this frequency, as can be seen in figure 4.5 for example, and since it is higher than the background by a significant margin (10^{14}), it is plausible that a pulse like this would still be picked up by the LOFAR antennas. However, because the pulses are only picked up above a frequency of 30 MHz, the signal is likely to be decreased by another factor of 10.

To answer the second question of how a phenomenon like this would look like in the data if it were to be measured, the data processing by LOFAR becomes important. A model like this produces radio waves in two pulses, namely when it speeds up and when it slows down. Intuitively, a prediction of two closely packed VHF sources would be the first guess. This might however not be how information like this is processed by LOFAR. The data processing makes the image slightly blurred and might mislocate a pulse. Because of this, it is difficult to predict how exactly a phenomenon like this would manifest in the data. At least two pulses would be visible in every step, but it can be more than two due to the data processing.

4.2 Streamer Collisions

Another model attempts to explain the emission of VHF radiation differently. Streamer collisions, as well as streamer propagation, are used to model the source of this radiation [15].
One thing a source of VHF radiation must have is a rapidly changing current. Like the previous model had a radio pulse emitted as the result of the stepping charge, the propagation and collisions of streamers have it too. Propagating streamers emit current pulses because they pick up charge while they propagate. Since the charge is changing, the current does so too. Hence, they exhibit a change in current and thus a current pulse. Collisions of streamers are a bit more intricate. It can most easily be visualized with the simulation results in figure 4.4.

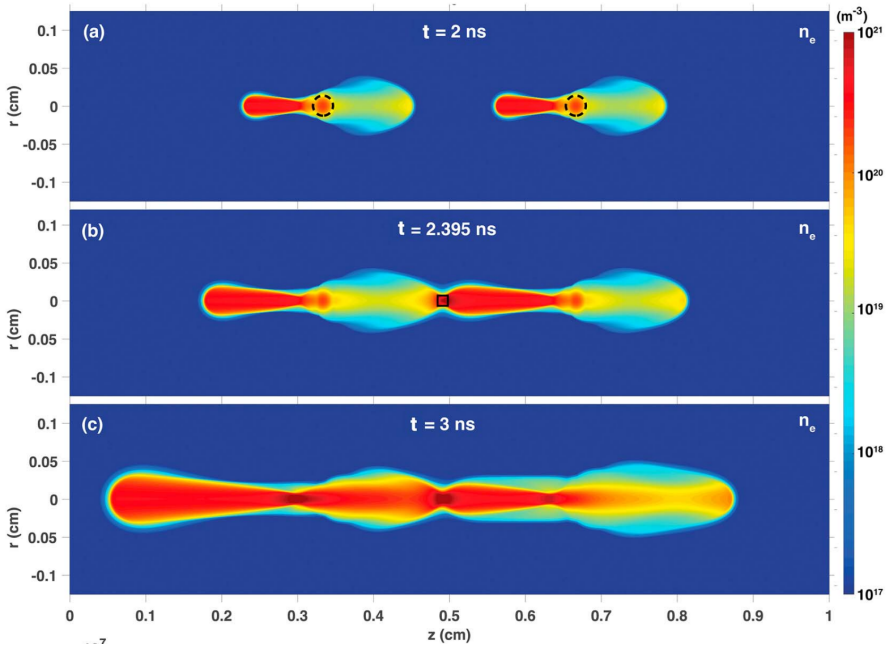

Figure 4.4: (a) Shows two streamers propagating bidirectionally before the collision. (b) During the collision, the electron density is enhanced in the region where the two streamers collide. (c) After the collision the streamers have merged into a single streamer [15].

As can be seen from figure 4.4, during the collision, the charge rearranges itself. The charge that is at the colliding tips, moves toward the ends to form a merged streamer. This rearranging charge means electrons are moving and thus a current is initiated. After the collision, the streamers merge into a single streamer and continue to propagate. So both the propagation and collisions of streamers exhibit rapid current pulses and thus could produce VHF radiation. The question remains if it indeed produces radiation in the range LOFAR is sensitive to. To answer this question, figure 4.5 can be used.

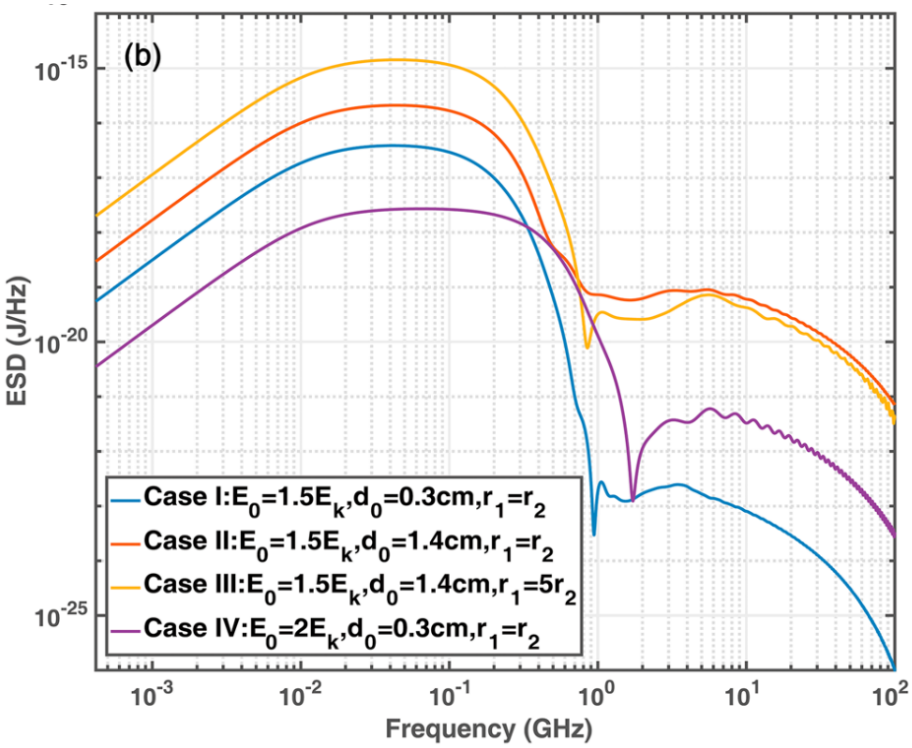

Figure 4.5: Showing the energy spectral density for the different simulation cases [15].

From this graph, it is clear in which frequency range these processes are most prominent. Namely, in the $10^{-2} - 10^{-1}$ GHz range, which does overlap with the range in which LOFAR operates ($30 - 80$ MHz). One last question remains: *How would a phenomenon like this look in the LOFAR data?*
According to this study, the electric field exceeds breakdown near the tip of the negative leader during corona flashes. This could cause negative streamers around the tip to collide with backwards travelling positive streamers. In the VHF range, the energy that is carried away from the negative leader is of the order of 10^{-8} J, which corresponds to about 10^6 streamers, assuming all streamers collide once. Since the amount of streamers and their collisions is so large, this would be a relatively long process, and thus it should produce VHF radiation over long periods. Hence, the data should show longer bursts of VHF radiation, which slowly dies off as the streamers collide and die off.

5 Results

In this section, the results obtained from the LOFAR data are analyzed. The temporal, as well as the spatial distribution, will be scrutinized. Lastly, the collected data will be compared to the two models discussed in section 4.1 and 4.2 to verify them and check how well they reproduce the measurements.

First, some general information about the plots will be discussed. Figure 5.1 shows a flash from 2017.

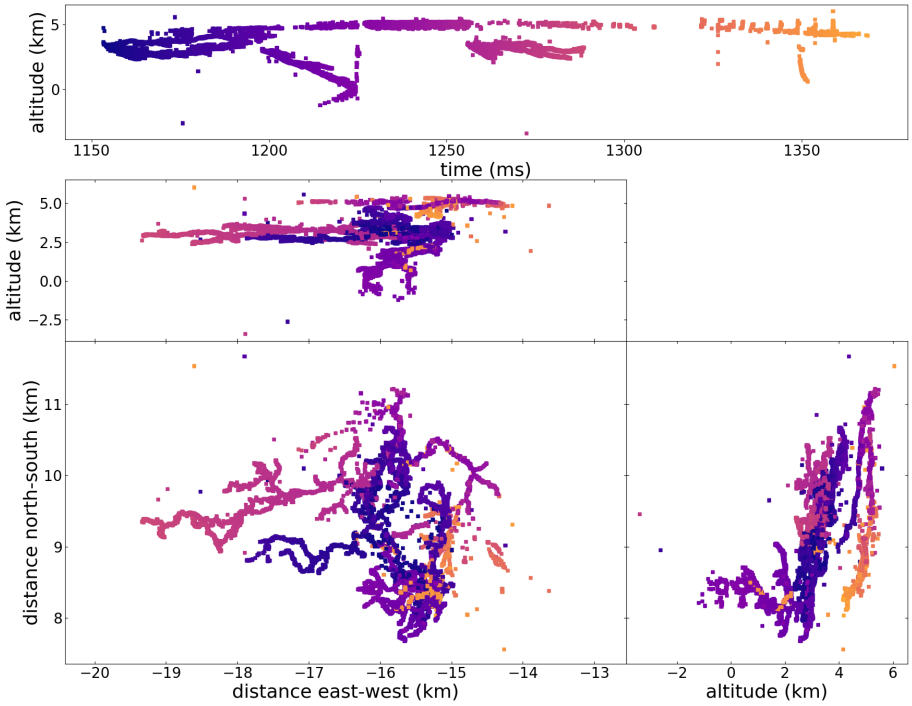

Figure 5.1: 2017 Lighting flash.

Each dot in figure 5.1 corresponds to a VHF source located in space and time. The top graph shows altitude versus time whereas the other graphs all show location in space. The colour of the dots indicates the passage of time, where the blue dots occur earlier than the purple dots, and the purple dots occur earlier than the yellow dots. This can be seen by the flow of colour in the top graph. The last important thing to note is that this graph shows negative leaders as well as positive leaders. This research will only focus on the negative leaders which, in this figure, typically occur below an altitude of 4 km. The height of the negative leader is about 4 km, and the leader moves over large distances so it is most likely at an angle to the antenna. Hence, on average the distance from the leader to the antenna is larger than 4 km, which is the reason why for the model in section 4.1, a distance of 7 km is used.

5.1 Temporal Distribution of a Negative Leader

The previous figure gives a clear impression of how the total flash is spread in space and time, but to examine the finer details of the negative leader, a closer look is necessary. Zooming in on the negative leaders reveals the finer structure.

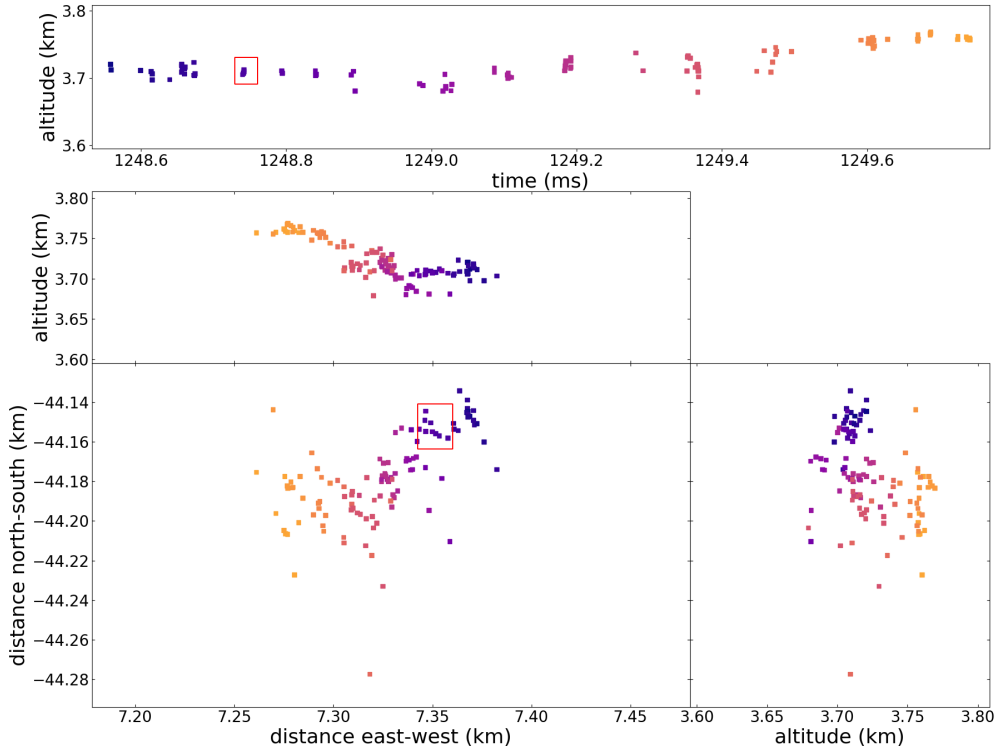

Figure 5.2: Negative leader from the 2018 flash.

Shown in figure 5.2 and in agreement with expectation, the negative leader does exhibit a stepping behaviour. This can be seen from the top panel in figure 5.2 where a step in time separates all sources. However, instead of single a VHF source for every step, clusters are visible. Every step contains a group of VHF sources. This can be seen by the closely packed groups of data points in each step of the leader. The presence of these clusters means there is not a single source of VHF emission, but multiple. The time separation between the bursts in figure 5.2 is of the order of tens to a hundred microseconds. A burst can contain more than five sources. Zooming in on the burst indicated in figure 5.2 reveals the following.

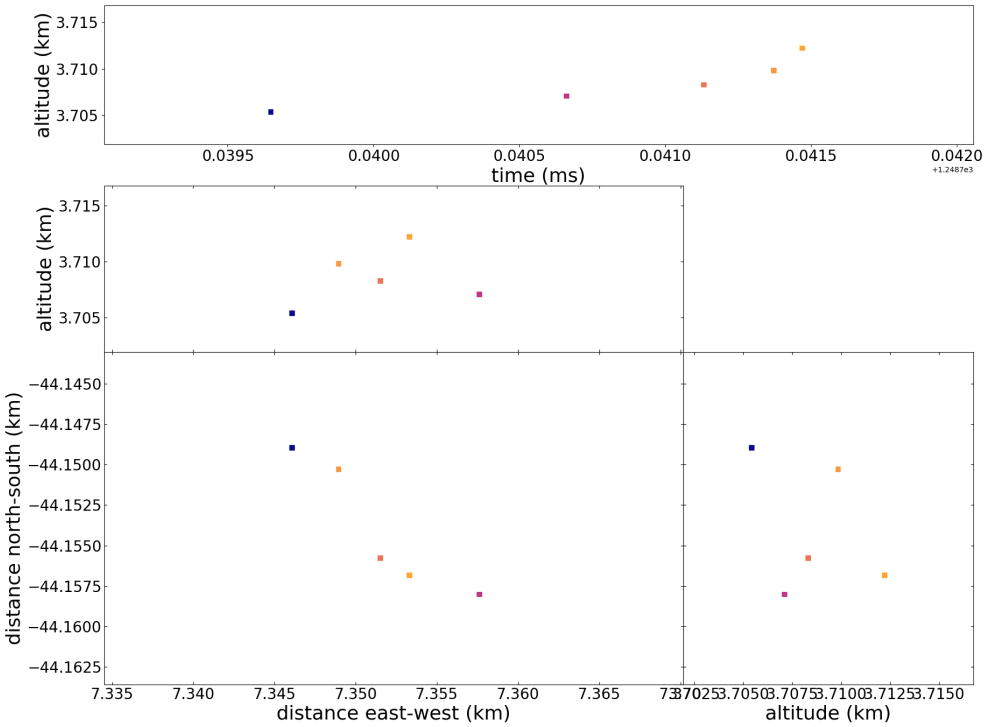

Figure 5.3: Zoom in on the burst of the negative leader.

In figure 5.3, it is visible that the sources are localized in time and space. The separation of the outer most sources in time is merely a few microseconds. In space, this burst is spread over around 20 m, in the shape of a line. This line lies along the negative leader channel. Most bursts in this negative leader follow this trend, with some variations. Temporal separation varies up to about 13 μs and the spatial separation up to 40 m. The raw data of the burst in figure 5.3 is shown in figure 5.4.

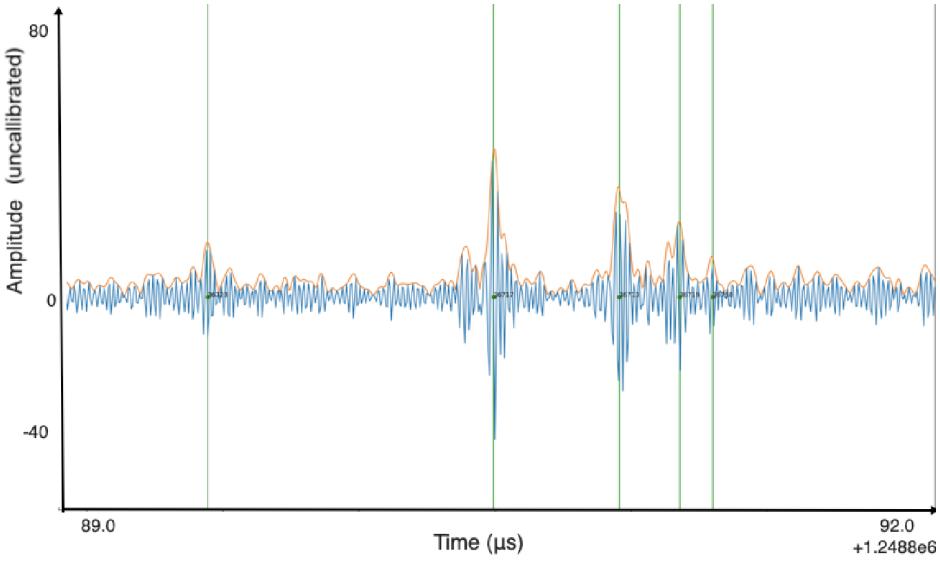

Figure 5.4: Raw data of the burst shown in figure 5.3.

In figure 5.4 it can be seen that there indeed are multiple pulses being measured. Also, the height of the pulses compared to the background can be estimated. Note that the pulses reach above the background by a factor of less than 10, note however, that the peak height in this graph is proportional to the electric field, not the electric field squared. The pulses in figure 5.4 are relatively weak. A pulse could reach out of the background by factors of 100 or even more, as demonstrated by figure 9.22 in the appendix. The width of the peaks indicates the time during which the pulse is emitted. From the graph a rough estimate can be made. The width lies in the nanosecond region which is why in section 4.1, 1 ns was taken for the value for τ.
Not all imaged negative leaders exhibit a clear stepping behaviour as in figure 5.2. An example of one is given in figure 5.5.

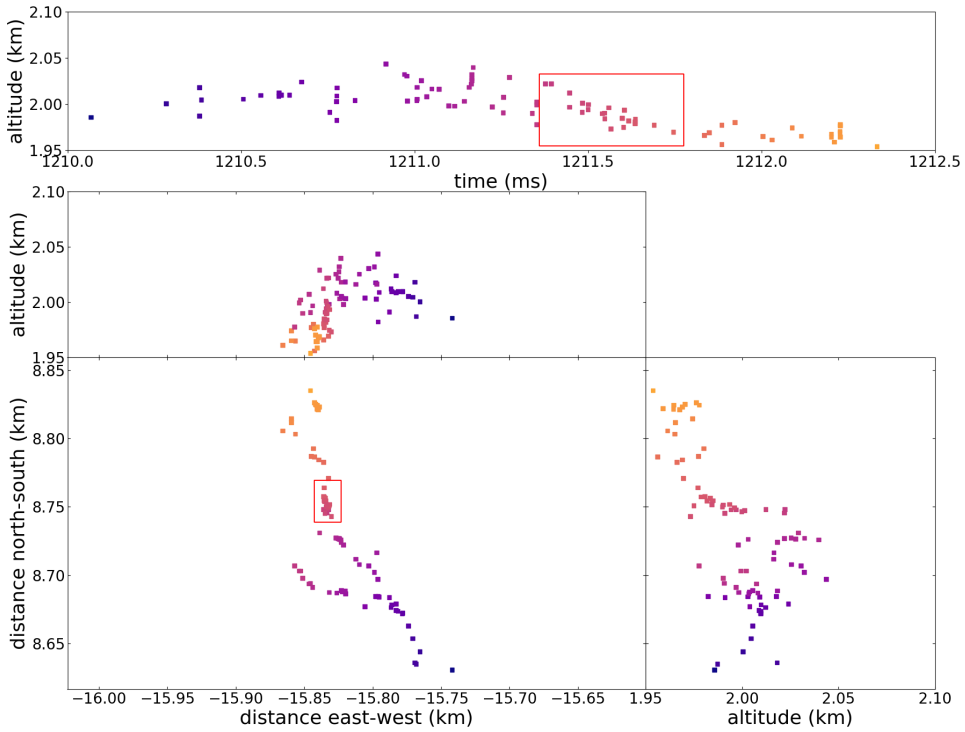

Figure 5.5: Another negative leader showing less clear stepping behaviour.

From figure 5.5, it is difficult to make up a stepping pattern. The propagation looks much more continuous than step-wise, also note that this leader is much closer to the ground. However, looking at the bottom graph reveals why it does not seem to step as the leader in figure 5.2 did. The bottom graph reveals branching in the main leader. Branching means that the main leader splits up, and multiple branches continue to propagate. All of these branches emit the same type of radiation at very similar times since they originate from the same main leader. Hence, if branching occurs, the stepping pattern becomes difficult to discern. However, some stepping can be seen by zooming in on the part of the main leader, indicated in figure 5.5. This area is chosen because no branching occurs here. The result can be seen in figure 5.6

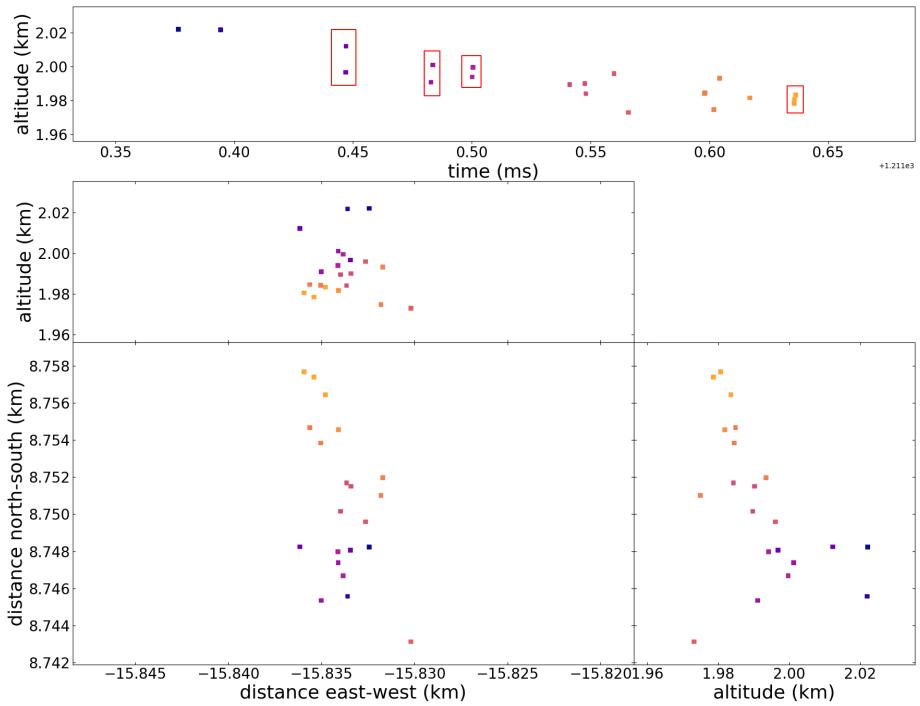

Figure 5.6: Zoom in on the main leader of figure 5.5.

The stepping is still a little blurred but there are a few bursts visible, as indicated in the figure. Although the stepping is less clear than in figure 5.2 it still behaves similar and emits bursts of VHF.

5.2 Spatial Distribution of a Negative Leader

To examine the spatial distribution, a different colour pattern is used. From the previous section, it can be seen that negative leaders exhibit a step-wise propagation in time, while emitting bursts of VHF radiation. The focus in this section will be to look at how the negative leaders move in space. To do this, each burst in the corresponding figure is given a specific colour such that it can be traced back to its location in space by looking for that same colour.

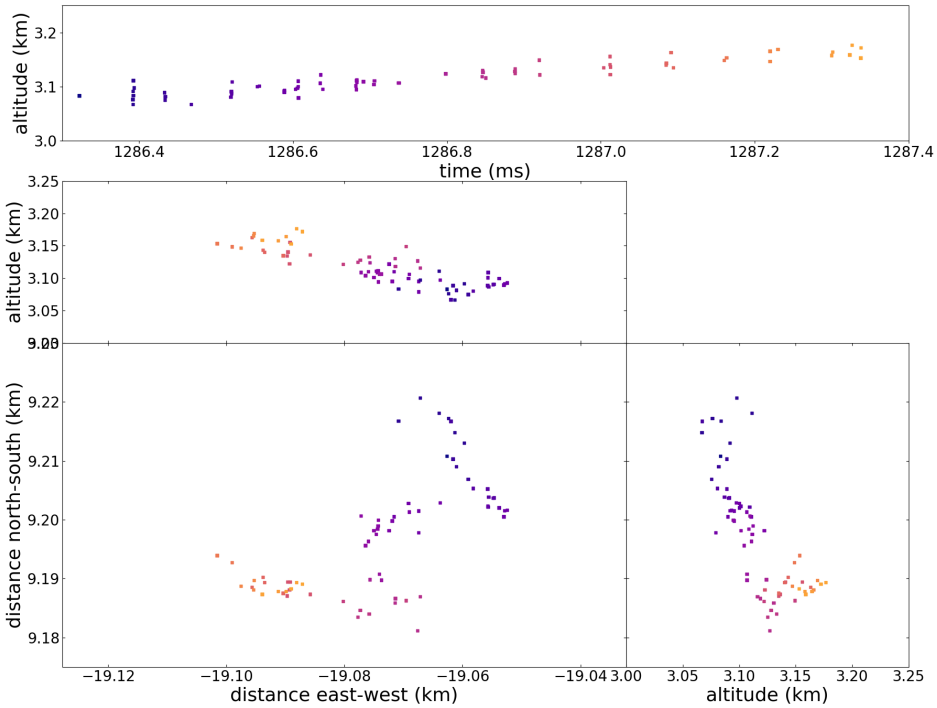

Figure 5.7: Negative leader from the 2017 flash, used to shown the spatial distribution of the bursts.

Note that in figure 5.7 the same colour pattern is used as before. To show the spatial distribution, smaller sections of this leader will be analyzed, to keep clear distinct colours. The leader in figure 5.7 will be analyzed in three sections, from left to right. The first, and thus outer left, section, is shown in figure 5.8.

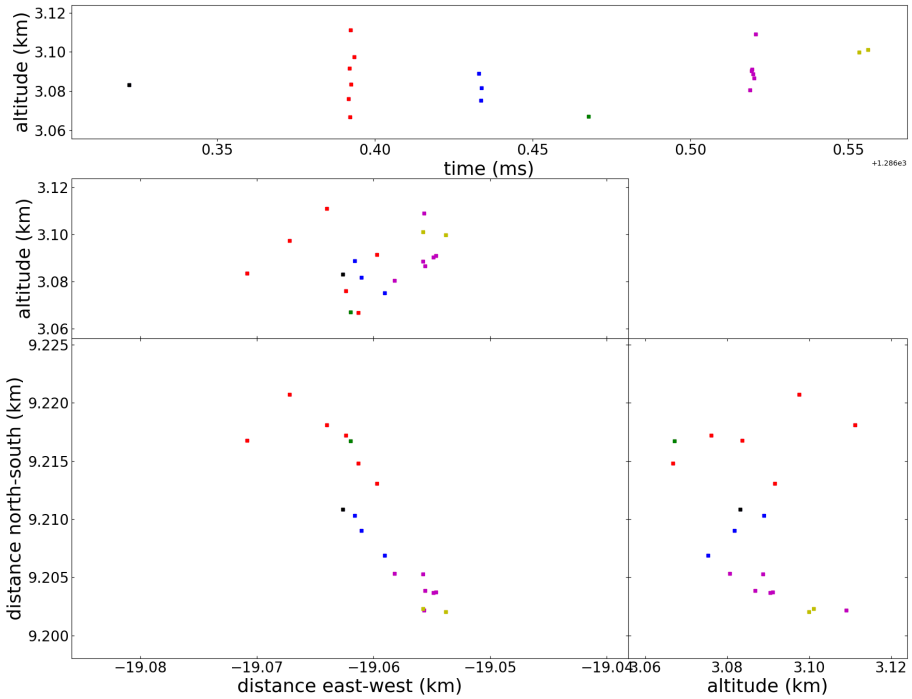

Figure 5.8: Zoom in on the outer left part of the leader shown in figure 5.7.

From figure 5.8, a clear stepping behaviour can be seen as well as bursts of VHF radiation. However, in space, it does not look step-wise. The leader first seems to propagate in the south-east direction, before turning around and propagate in the north-west direction. Also, the bursts that are seen in the temporal distribution are not observed. The bursts are spread over areas comparable to the length of a step, since one burst can overlap with the next. Although stepping is difficult to discern, the leader does propagate. The average location of the spread out bursts does move. The separation in space of these bursts is of the order of 10 m.

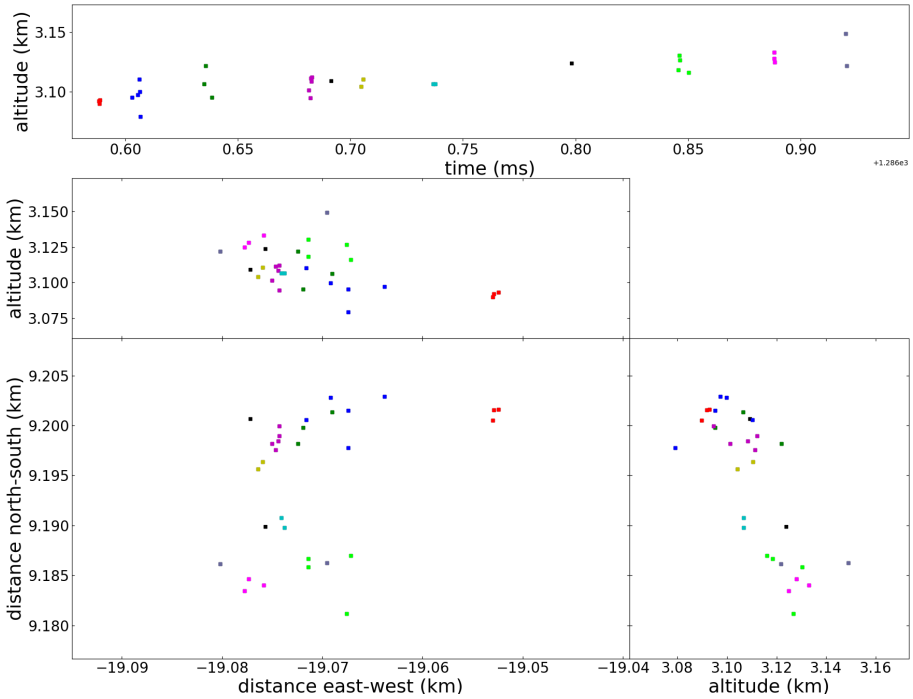

Figure 5.9: Zoom in on the middle of the leader shown in figure 5.7.

In figure 5.9 the second section is displayed. Stepping in time is clearly visible here. Also, propagation in space is clearer. The bursts still overlap but the propagation does not seem as continuous as in the first section. Also, for this section the propagation direction is very clear. It propagates in the north-east direction. The step length is of the order of $5 - 10$ m.

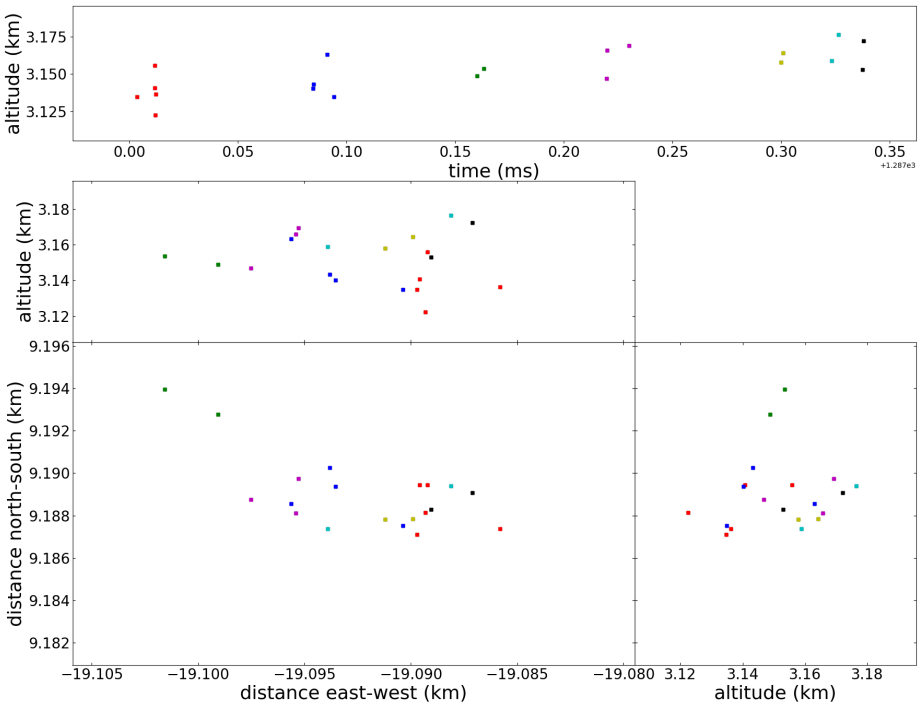

Figure 5.10: Zoom in on the outer right section of the leader shown in figure 5.7.

For the last section, again, a clear stepping behaviour in time is observed. However, the propagation is space is unclear. The initial and final points are at the same location in the bottom left panel but differ in altitude slightly. Implying the leader made a 180° turn and went back to the starting position, with a slight change in altitude. The step length is again of the order of $5 - 10$ m with overlapping bursts. Additional data is given in the appendix but left out of the results to maintain readability.

5.3 Comparing Models to the Obtained Data

Now, the models discussed in section 4.1 and 4.2 will be compared to the data to validate how well they reproduce the measurements. Firstly, a summary of what has been found in the data. As can be seen in section 5.1 and 5.2, clear stepping behaviour in time has been found. This means VHF radiation is observed in evenly spaced intervals. These intervals are of the order of $40 - 100$ μs. Besides the temporal stepping behaviour, the data shows clusters of VHF sources at every step. So, instead of one source per step, there are multiple, which are localized in time. The temporal separation of pulses inside these bursts are merely $2 - 15$ μs. In space, the bursts are spread over a distance of about $2 - 10$ m. The stepping in space is observed less clearly, but the distance between bursts are of the order of 10 m. It also shows that the radiation is emitted along the step of the leader.

To validate the models, it should be checked how well they reproduce these results. Starting with the model discussed in section 4.2, the streamer propagation and streamer collisions.

As discussed in that section, a large amount of streamers have to be produced to accommodate for the energy that is carried away by the observed VHF radiation. This number of streamers is of the order of 10^6. The collisions and propagation of all these streamers will take some time to die off. In the data, a burst only lasts for up to 15 microseconds. If streamer collisions and streamer propagation were the sources of this radiation, the bursts would last longer in time. Thus, this model does not reproduce the measurements very well.

The model discussed in section 4.1 has other problems. First of all, it predicts bursts with a smaller amount of sources than the data shows. Secondly, the resulting power from that model is of the order of 10^4 W. The background is an order of 10^{16} lower. This gap will be reduced by a decrease in antenna sensitivity at large zenith angles, bringing the difference back to a factor of 10^{14}. Also, since LOFAR only measures radiation that is higher than 30MHz, and the pulse has maximum intensity at 5MHz, the power could decrease by another factor of 10. However, in the measurements, peaks with this height are not seen. As demonstrated in figure 5.4, the peaks are a factor of 10 to 100 higher than the background. Note however, that this data is proportional to the electric field, not the electric field squared. To compare this data to the power output, the square root of the difference should be taken. The gap between power output and background is 10^{14}, so the difference in peaks would be about 10^7. This is still a large gap with what is measured. The simplicity of this model can not be wrong, but the discrepancy between emitted and observed power is strong evidence against this model, thus hinting at a different mechanism that is responsible for the measured radiation.

6 Discussion

In this research, the propagation of negative lightning leaders is studied. According to expectations, they propagate step-wise. In time, clear steps are visible, although in space the leader propagates more continuously. Steps in space can still be seen but the bursts are more spread out in space than in time. This behaviour is seen in the majority of the negative leaders. In some negative leaders, the spatial propagation is more difficult to discern, figure 9.2 for example.
Instead of single pulses of VHF, they emit bursts for every step, see figure 5.2. Multiple sources of VHF radiation did not lie in line with expectations, but is visible on all the negative leaders. Currently, it is unknown what causes these bursts. Two models were discussed in section 4.1 and 4.2. The model concerned with streamer propagation and collisions can be ruled out because it predicts elongated bursts of VHF emission, while the data shows very short bursts. The model with the accelerated charge has different problems and hints at a different mechanism. First of all, it predicts two pulses inside a burst, but bursts with more than five sources are found in the data. Also, according to calculations, the accelerated charge would emit a power of $P = 4.8 \cdot 10^4$ W. Comparing this to the background of about 10^{-12} W, the conclusion is that it would certainly reach above the background. The measurements however do not reveal peaks of this height. The discrepancy between measured peak heights and the prediction from this model is of the order of 10^7.

There are a few areas in which the problem with this model can lie. The simplicity of this model can not be wrong, so it has to be one of the parameters or assumptions that have been made. The speed of a negative leader could be much lower during the step, which causes a lower current to run. However, this might only make a difference of a factor of 10. Also, the charge might not be localized perfectly in the tip, but spread out over a larger length along the leader. A spread out charge, making the same step would emit less power, and thus result in a lower peak. One other explanation could be that instead of one current pulse, multiple smaller current pulses occur. This would correctly predict bursts with multiple data points and also decrease the height of the peaks. The peak height would decrease since a current pulse with a smaller charge emits less power. To correctly predict the peak height, a charge of about 1 μC should be taken. This would mean about 1000 smaller currents run during one step. But in the data only a handful are visible. So clearly this does not solve all the problems with this model. Note that a charge of 1 μC comes close to the charge of a streamer [16]. So streamers could be the source of this radiation after all. Only a smaller number than is predicted by the streamer propagation and collisions model.
If the negative leader takes a step, suddenly the potential in the surrounding area the leader moves in to, changes rapidly. This sudden change in potential could cause streamers to emerge and start to propagate. Looking at the structure of a burst, it can be seen that for most bursts, the sources of radiation are formed in a line along the negative leader channel.

This does conform with the idea that streamers are formed along the negative leader when it takes a step. Besides, the sources that form this line, do not form a line with a chronological order, but the time for each pulse seems random. That can be explained by the fact that the start electron avalanches is a somewhat random process and thus the order that these avalanches start in, do not have to follow the order of the lines seen in the data. However, not all bursts look like this. Some do not form a line along the leader channel, see figure 9.11 and 9.18 for example. More research into the exact structure of these bursts is needed to correctly model the mechanism behind the emission of VHF in lightning leaders.

7 Conclusion

During this research, the data obtained by LOFAR was used to scrutinize the propagation of negative lightning leaders. Lightning leaders emit VHF radiation, which is measured by LOFAR. The mechanism responsible for this VHF emission is currently unknown. Some of the obtained data is shown in the results section and the appendix. Three features can be made up of the obtained data.
Firstly, the VHF radiation is emitted in distinct steps. This is in line with the understanding of how negative laboratory sparks propagate, namely, in a step-wise fashion.
Secondly, instead of single pulses, the leader emits bursts of VHF radiation at every step. This was not in line with expectations. A burst of VHF radiation in a single step means that in a single step there are multiple sources of radiation.
Thirdly, the propagation in space is not step-wise. In space, the leader propagates more continuously, with bursts overlapping. On average, the location of the bursts does change. For these properties, the following values were obtained from the data:

- Stepping time: $40 - 100$ μs
- Stepping length: $5 - 10$ m
- Spatial separation of a burst: $2 - 10$ m
- Temporal separation of a burst: $1 - 10$ μs

Two models for the emission of VHF radiation were discussed. The first model, explaining the emission of VHF through an accelerated point charge gives a predicted power output that is much higher, a factor of 10^7, than the background. Measurements do not show peaks with this height and thus, this model does not reproduce the measurements well. Streamer collisions and streamer propagation were other candidates for the emission of VHF radiation. However, this model does not reproduce the LOFAR measurements. According to this model, VHF radiation would be emitted over a longer time than the found $1 - 10$ μs. Thus, this model can be ruled out.
To conclude, the obtained data from LOFAR shows in addition to the expected stepping behaviour, unexpected bursts of VHF radiation for every step. The two discussed models do predict features of the data correctly, but are not able to reproduce it fully. Hence, more research into this subject is needed to model this phenomenon correctly.

8 Bibliography

[1] J. R. Dwyer and M. A. Uman, *The physics of lightning.* Physics Reports 534, 2014.

[2] I. Gallimberti, G. Bacchiega, A. Bondiou-Clergerie, and P. Lalande, *Fundamental processes in long air gap discharges*, 2002.

[3] E. R. Williams, "The electrification of thunderstorms," *Scientific America*, 1988.

[4] G. F. Knoll, *Radiation Detection and Measurement.* John Wiley and sons Inc., 2000.

[5] A. M. Romero and A. Luque, "Spontaneous emergence of space stems ahead of negative leaders in lightning and long sparks," *Geophysical Research Letters*, 2019.

[6] M. P. van Haarlem *et al.*, "Lofar: The low-frequency array," *A and A*, vol. 556, 2013.

[7] A. S. Cohen *et al.*, "The vla low-frequency sky survey," *The Astronomical Journal*, vol. 134, 2007.

[8] W. M. Lane *et al.*, "Vlss redux: Software improvements applied to the very large array low-frequency sky survey," *Radio Science*, vol. 47, 2012.

[9] J. J. Condon *et al.*, "The nrao vla sky survey," *The Astronomical Journal*, vol. 115, 1998.

[10] M. de Vos, A. W. Gunst, and R. Nijboer, "The lofar telescope: System architecture and signal processing," *Proceedings of the IEEE*, vol. 97, no. 8, 2009.

[11] C. Tasse, B. van der Tol, J. van Zwieten, G. van Diepen, and S. Bhatnagar, "Applying full polarization a-projection to very wide field of view instruments: An imager for lofar," *A and A*, 2012.

[12] J. Howard, M. A. Uman, C. Biagi, D. Hill, V. A. Rakov, and D. M. Jordan, "Measured close lightning leader-step electric field–derivative waveforms," *Journal of geophysical research*, 2011.

[13] K. Mulrey *et al.*, "Calibration of the lofar low-band antennas using the galaxy and a model of the signal chain," *The Astronomical Journal*, vol. 115, 2019.

[14] W. van Cappellen, M. Ruiter, and G. Kant, "Low band antenna architectural design document," *Public*, 2007.

[15] F. Shi, N. Liu, J. R. Dwyer, and K. M. A. Ihaddadene, "Vhf and uhf electromagnetic radiation produced by streamers in lightning," *Geophysical Research Letters*, 2018.

[16] R. Morrow and J. J. Lowke, "Streamer propagation in air," *Journal of Physics D: Applied Physics*, vol. 30, no. 4, 1997.

[17] V. Cooray and L. Arevalo, *Modeling the Stepping Process of Negative Lightning Stepped Leaders*, August 2017.

[18] A. Chilingarian, S. Chilingaryan, T. Karapetyan, L. Kozliner, Y. Khanikyants, G. Hovsepyan, D. Pokhsraryan, and S. Soghomonyan, "On the initiation of lightning in thunderclouds," *Nature*, 2017.

[19] R. HASBROUCK, "Mitigating lightning hazards," *Science and Technology Review*, 2013.

[20] M. A. Uman, K. Mclain, and E. P. Krider, "The electromagnetic radiation from a finite antenna," *American Journal of Physics*, 1975.

9 Appendix

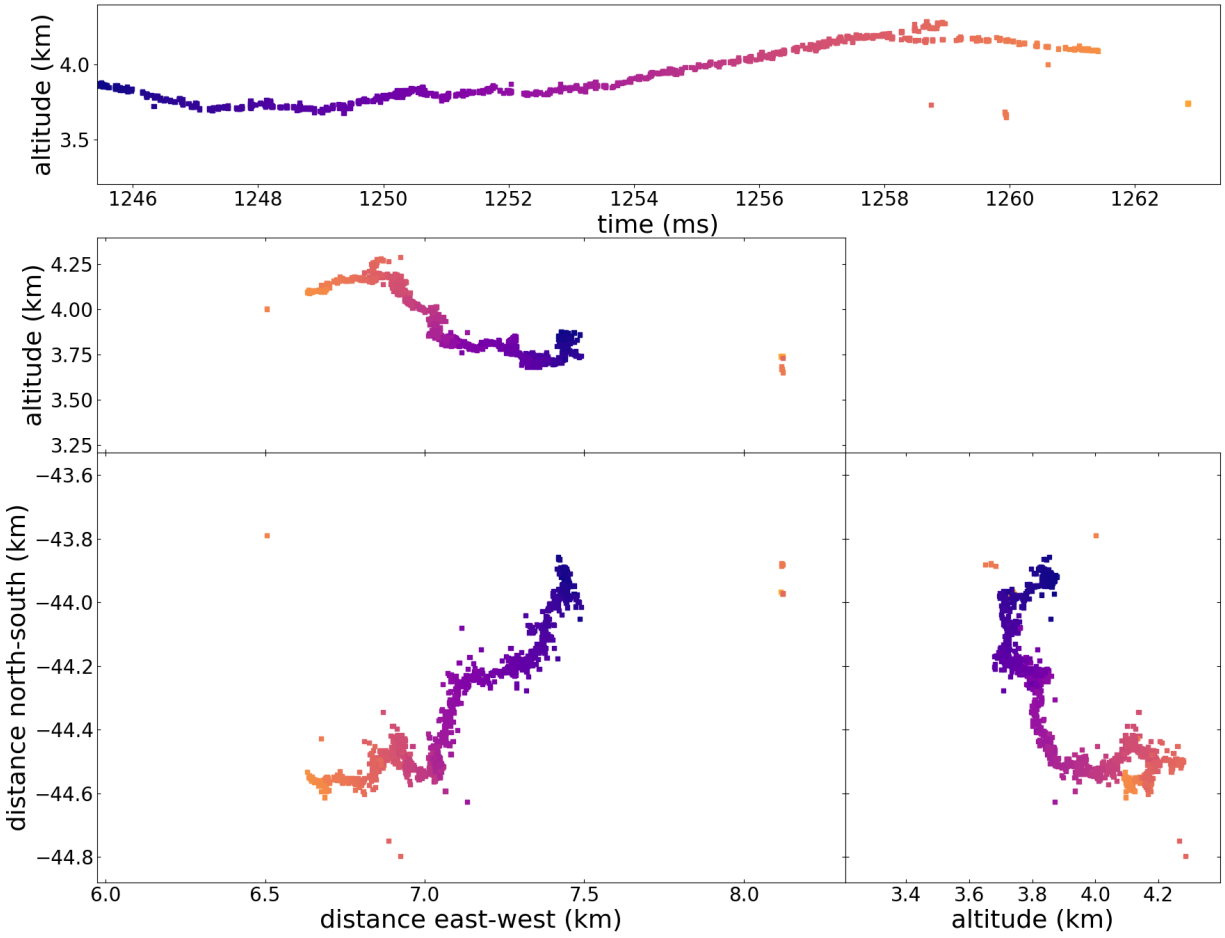

Figure 9.1: A Negative Leader from the 2018 flash.

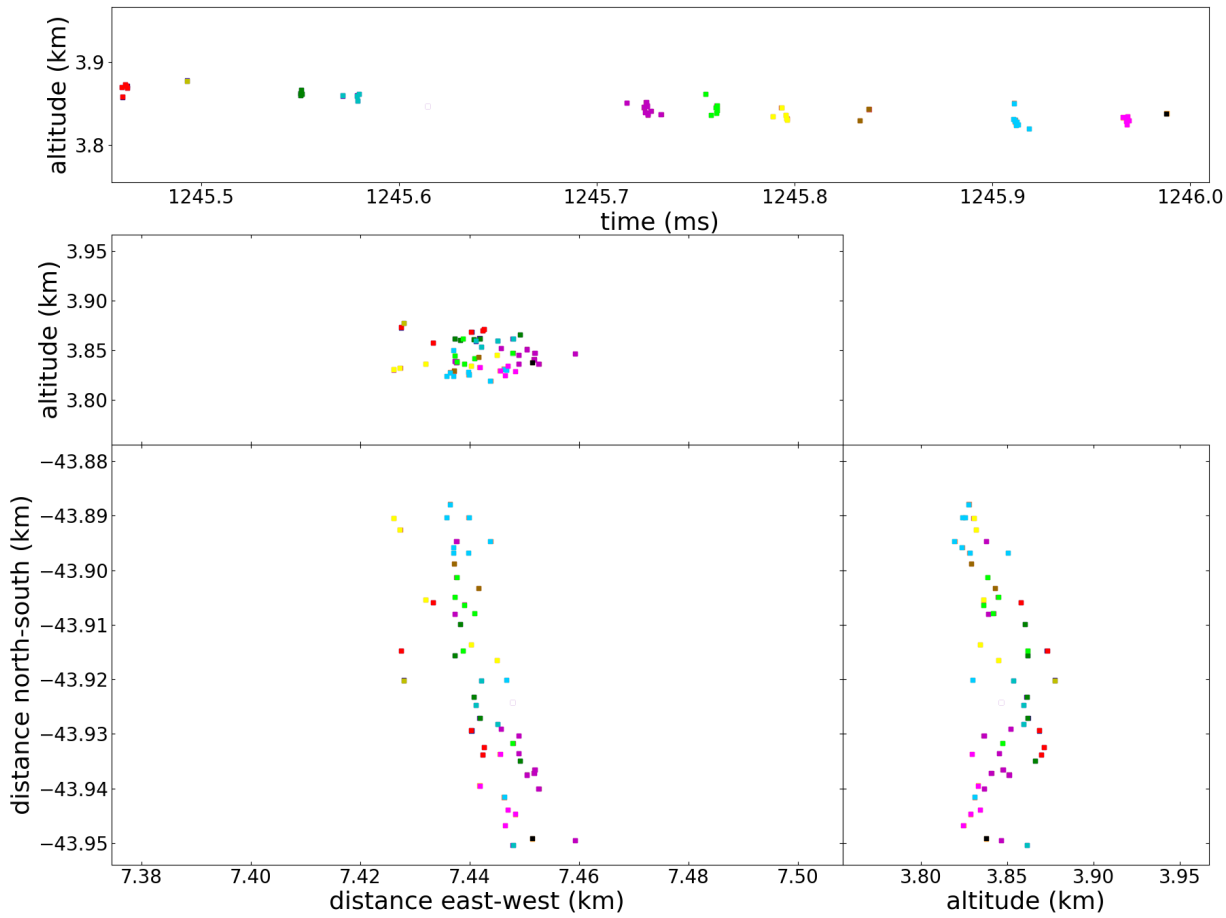

Figure 9.2: A zoom in on the negative leader shown in figure 9.1.

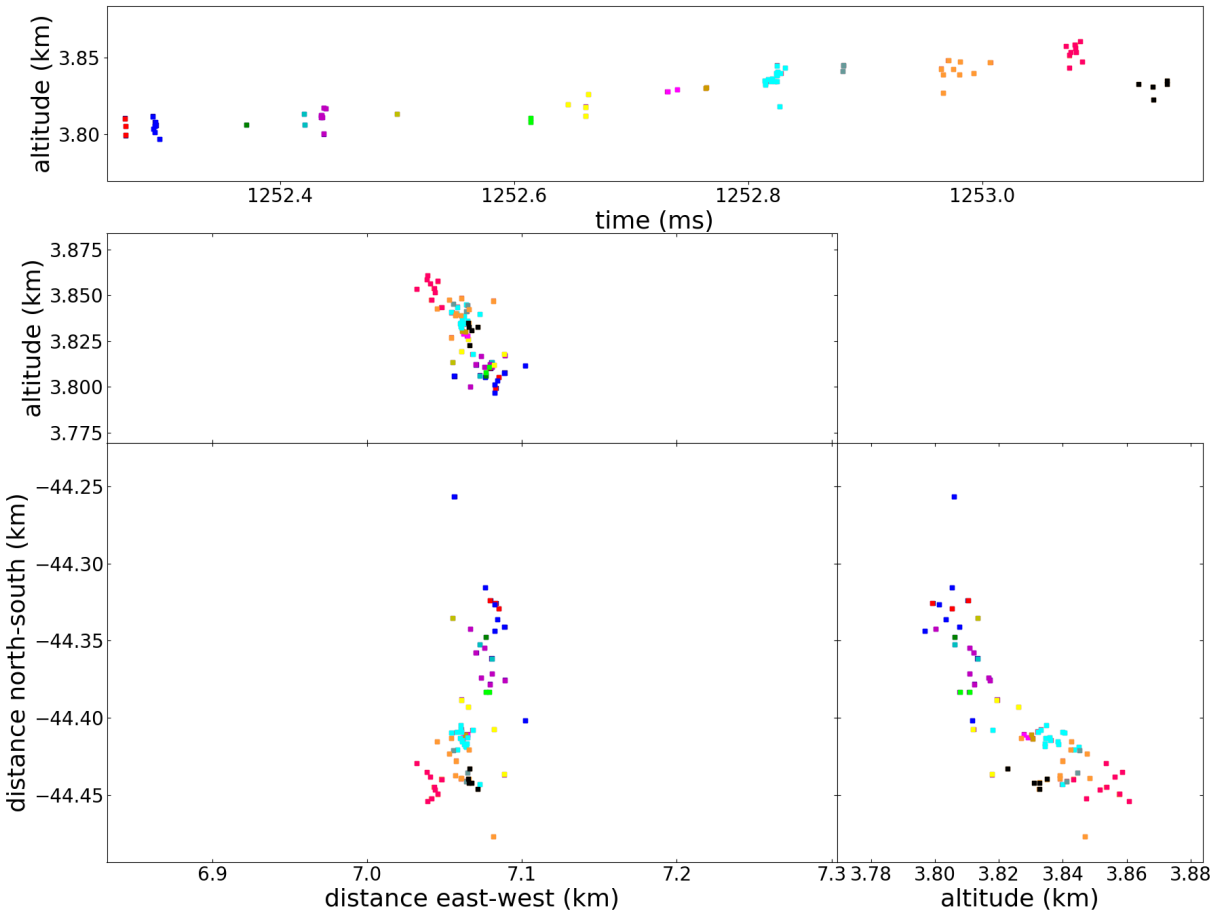

Figure 9.3: Second zoom in on another area the negative leader from figure 9.1.

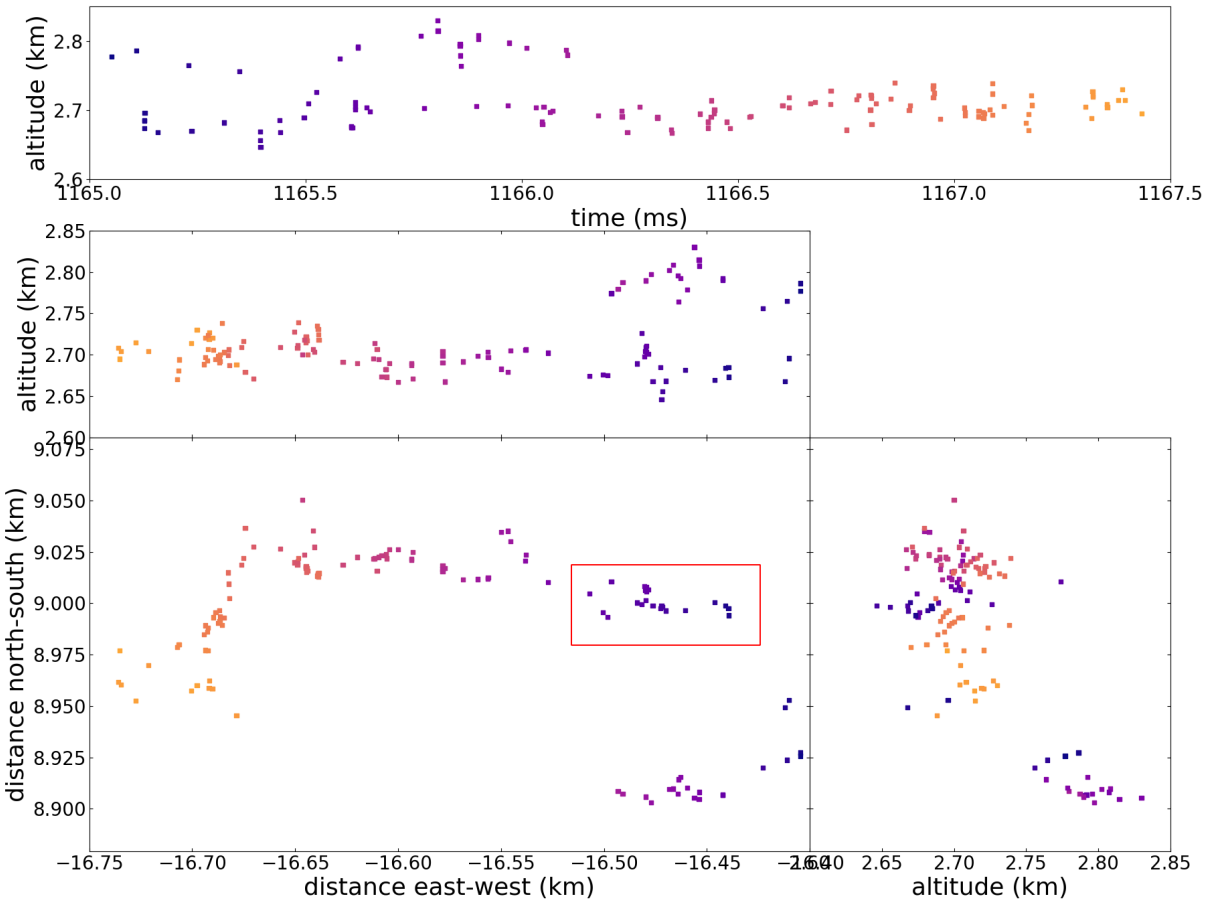

Figure 9.4: A Negative Leader from the 2017 flash. In red indicated which area is taken to be zoomed in on.

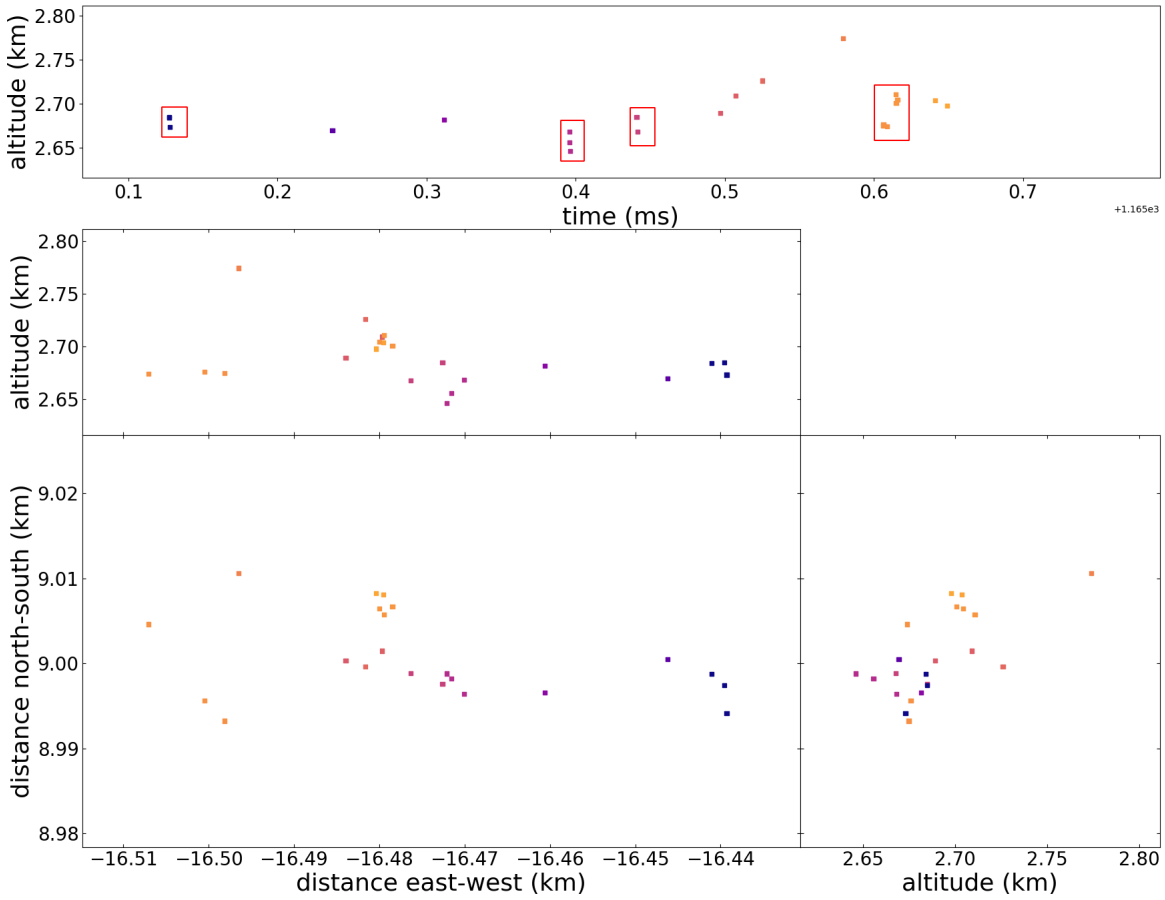

Figure 9.5: Zoom in on the indicated area of the negative leader in figure 9.4. The red boxes indicate clearly visible bursts.

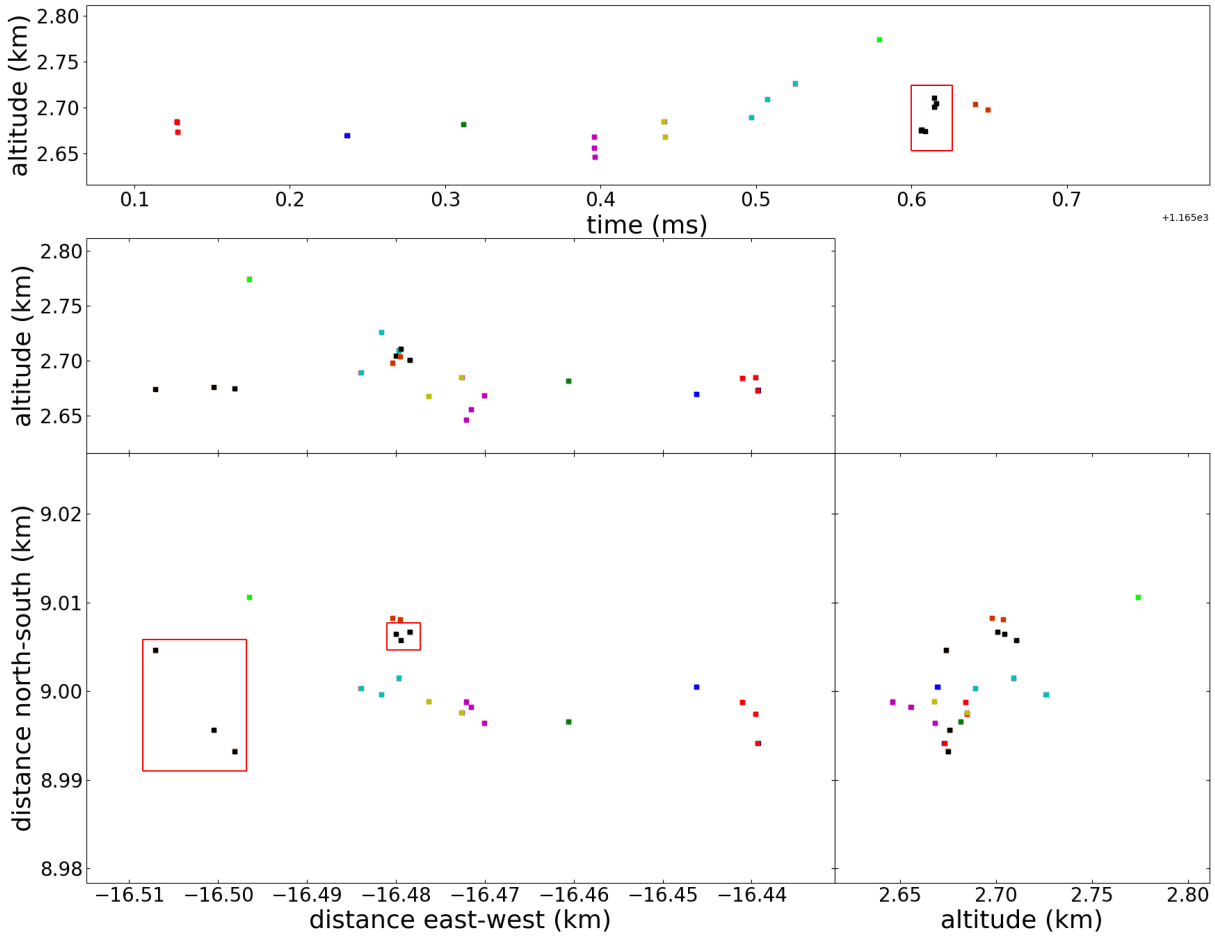

Figure 9.6: The same zoom in of the leader in figure 9.4, but the with the alternate colour pattern. This shows the propagation in space more clearly. The boxes indicate the black burst being separated in space. Meaning the black burst is actually not a single burst, but two occurring at the same time.

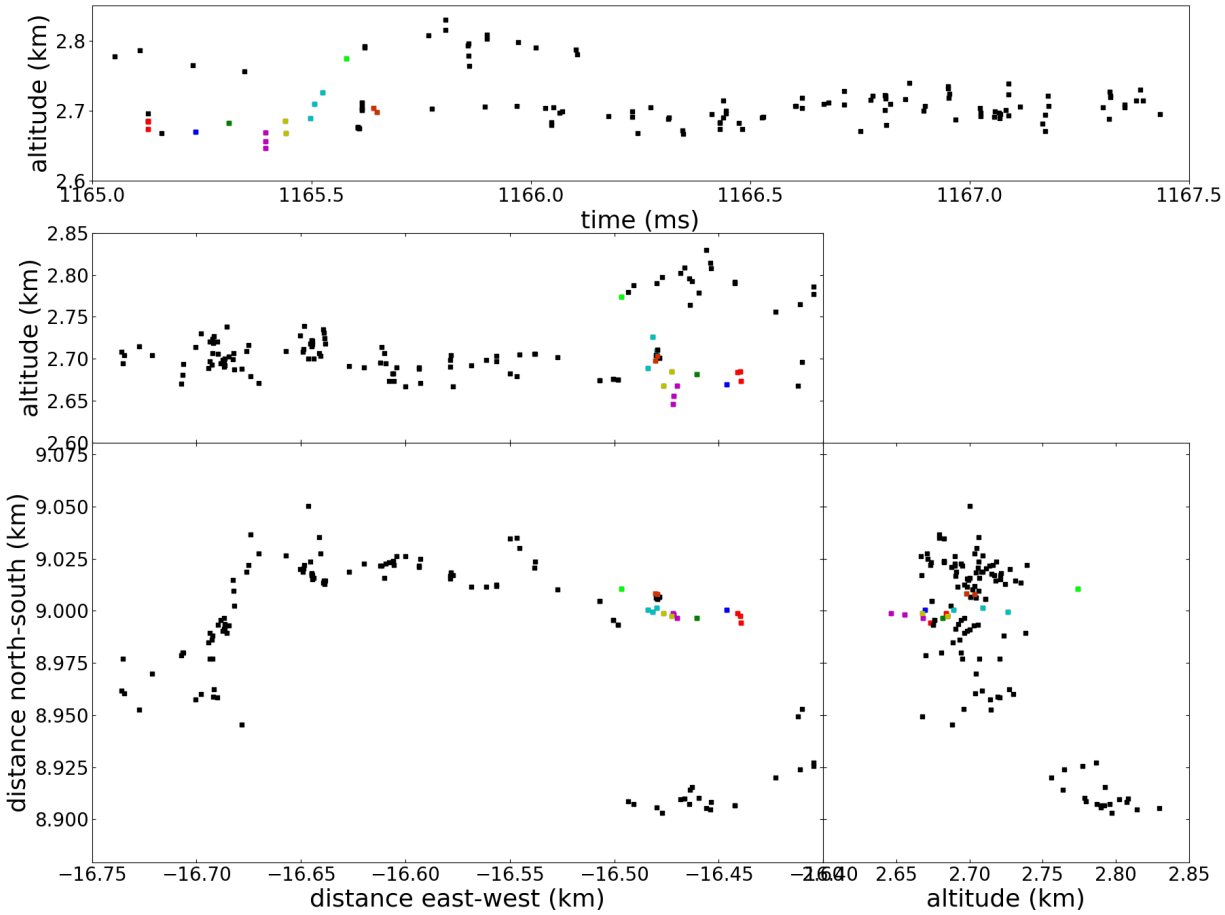

Figure 9.7: A zoomed out image of the leader in figure 9.4 to show it on a slightly larger scale. This clearly shows the leader branches into two segments.

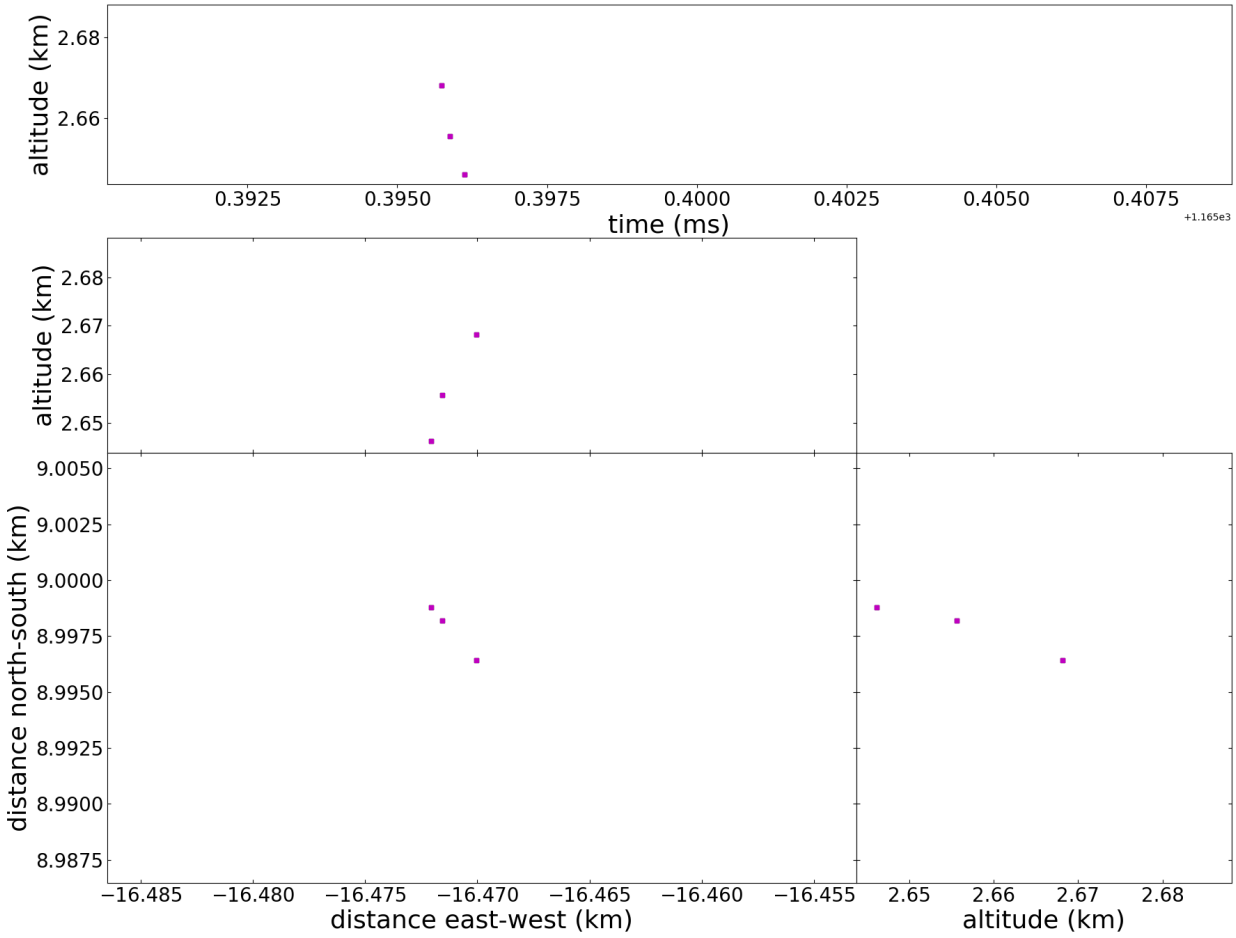

Figure 9.8: A zoom in on the magenta burst in figure 9.6

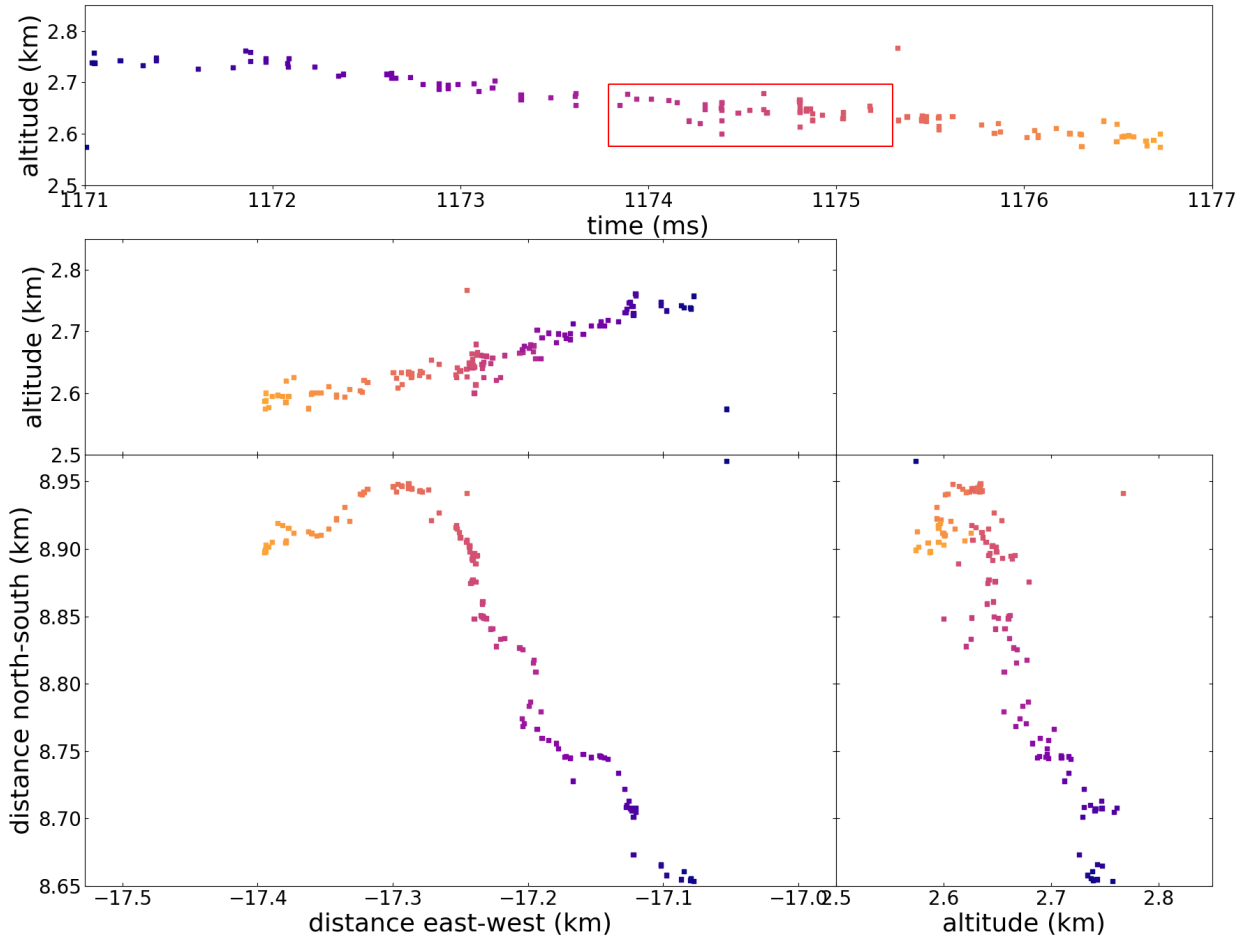

Figure 9.9: A different negative leader from the 2017 flash. The red box indicates the area on which will be zoomed in.

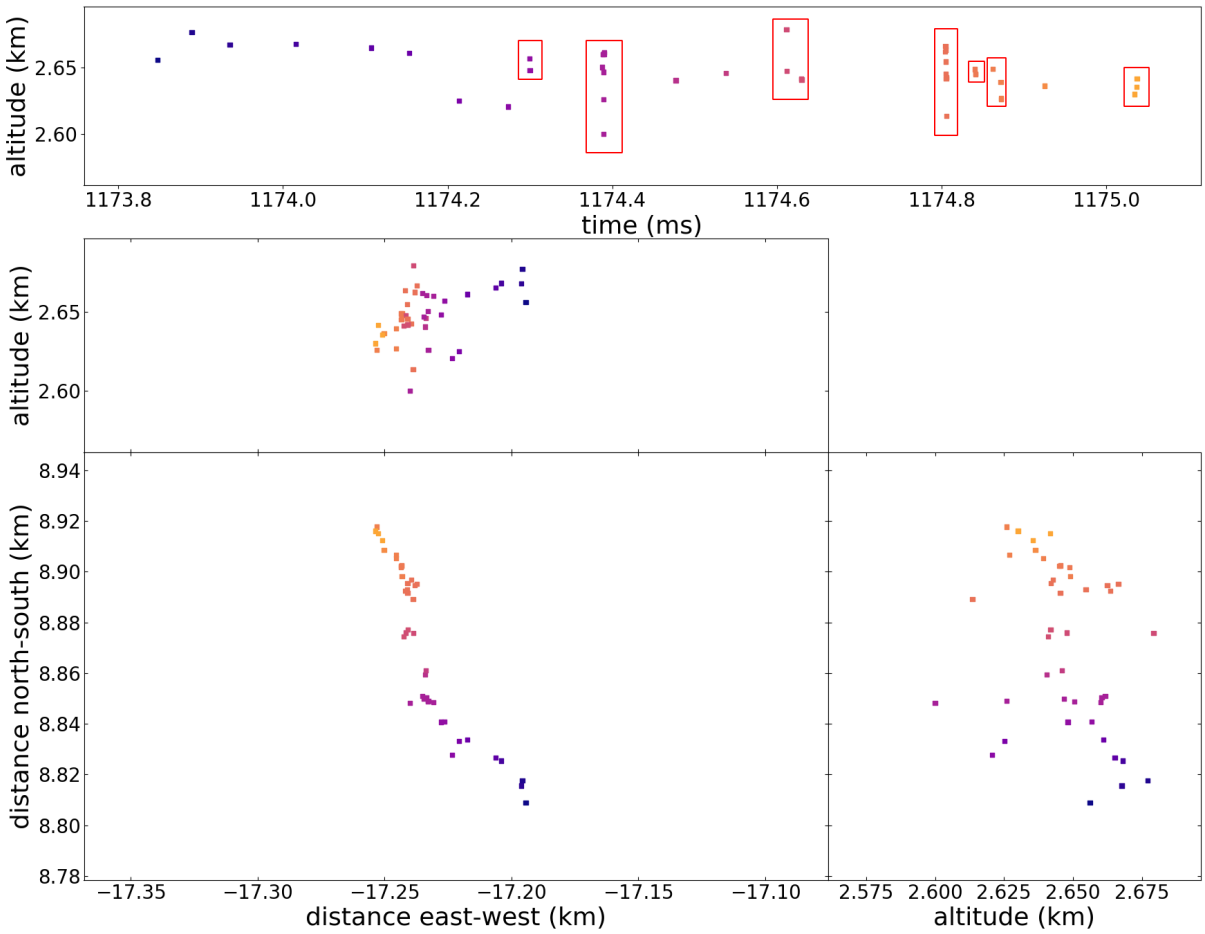

Figure 9.10: Zoomed in image of the leader shown in figure 9.9. The red boxes indicate the clearly visible burst along this stretch of the leader.

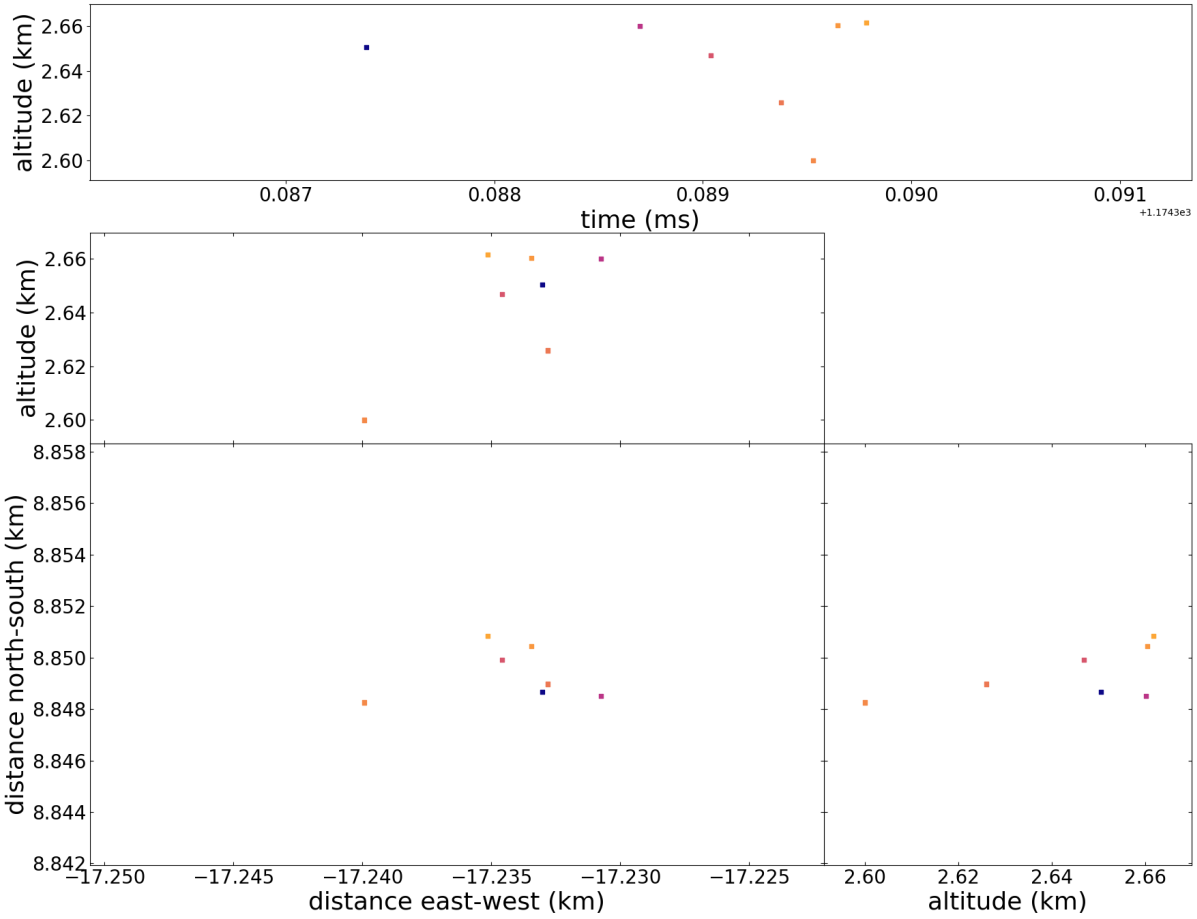

Figure 9.11: Zoom in on the burst indicated by the second red box from the right in figure 9.10.

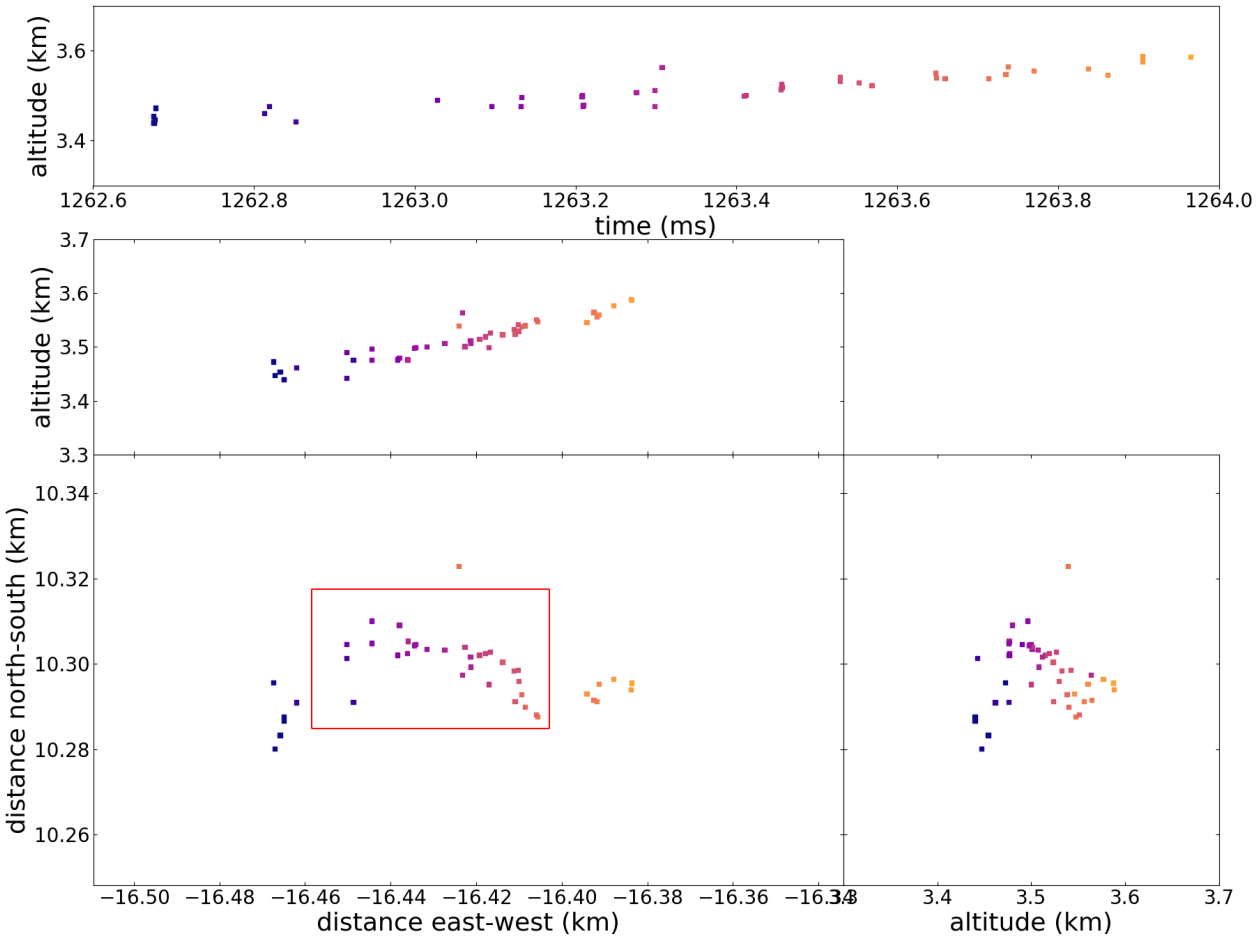

Figure 9.12: Another negative Leader from the 2017 flash. The red box indicates the area that will be zoomed in on.

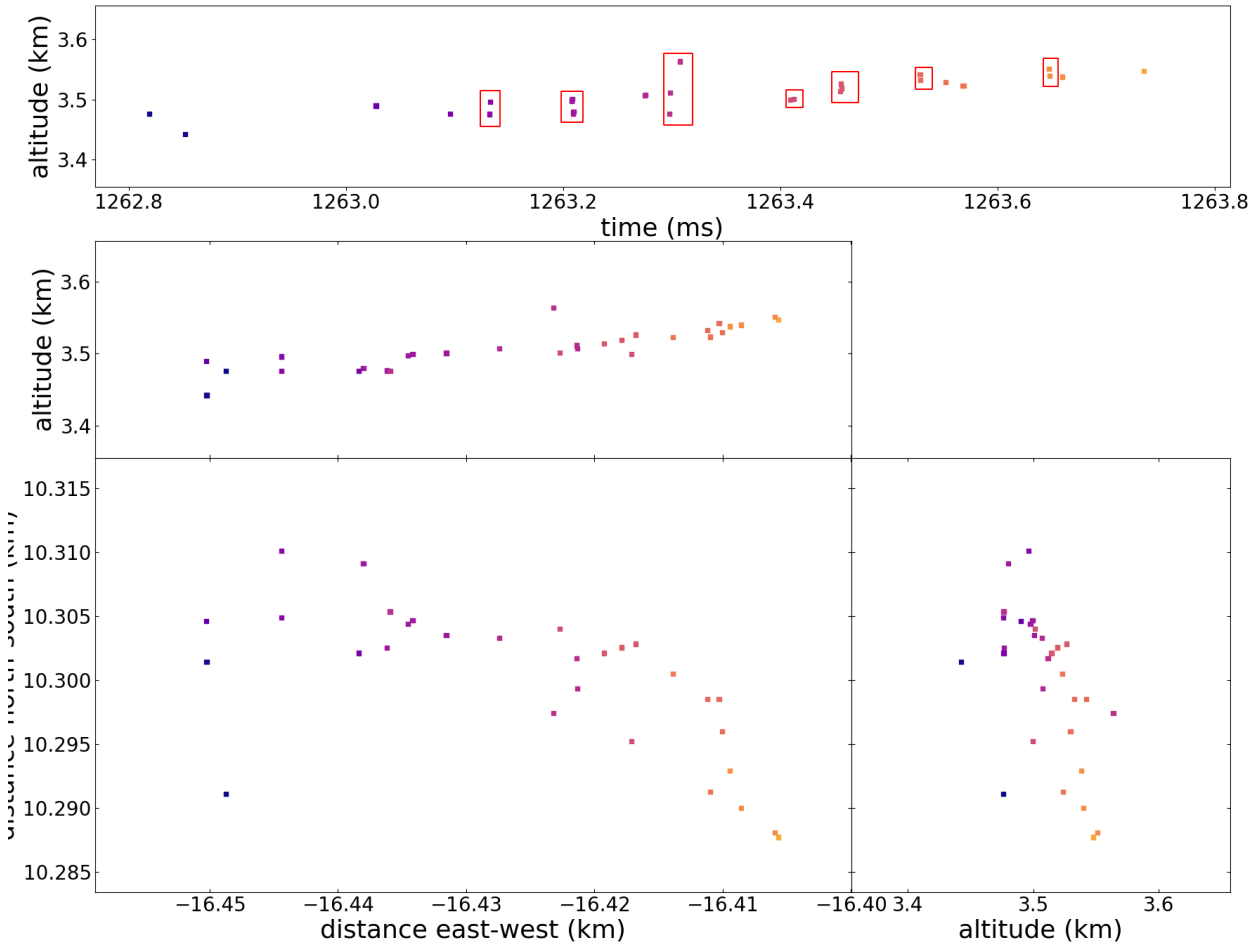

Figure 9.13: Zoom in of the leader from figure 9.12. The red boxes indicate the visible bursts.

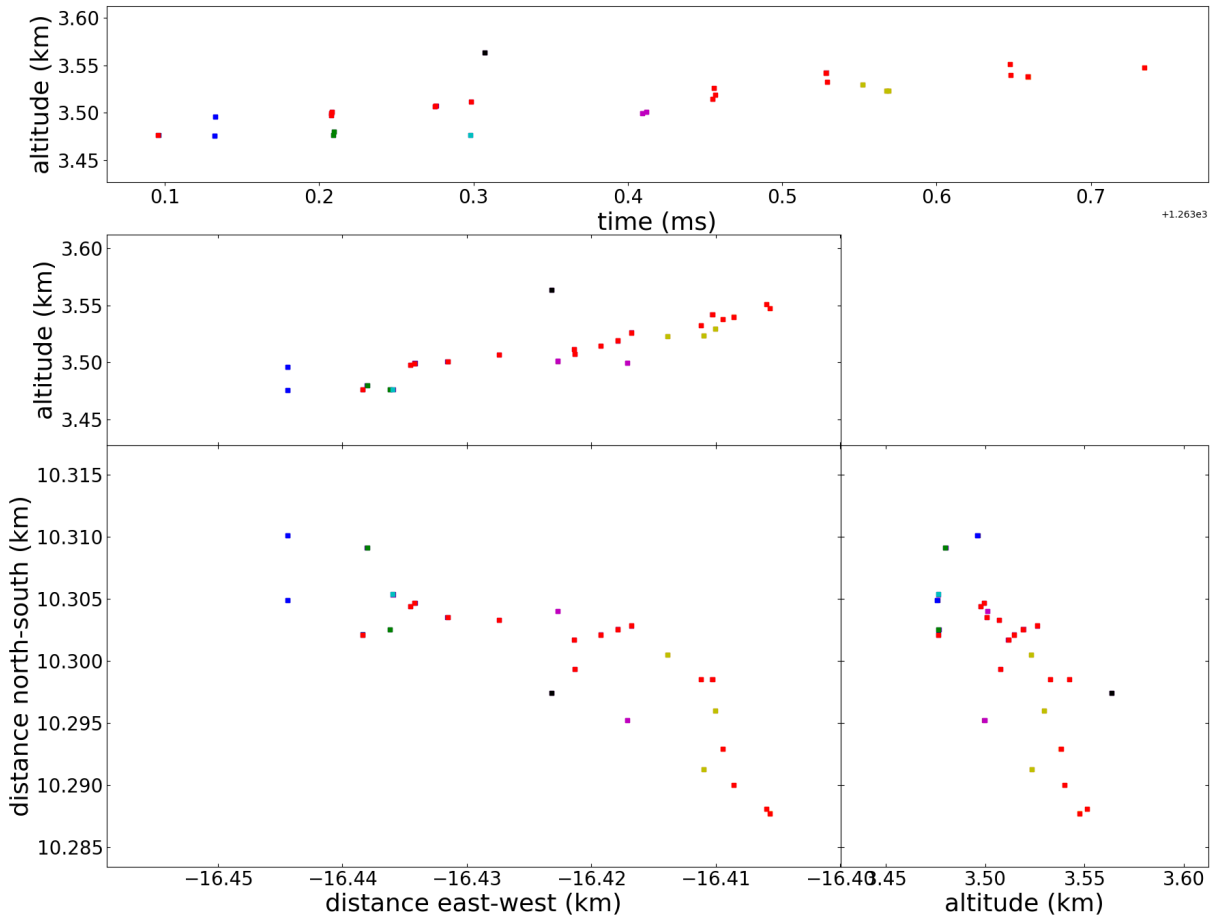

Figure 9.14: Showing the same section of the negative leader from 9.12, but with the alternate colour pattern. Here the propagation in space becomes more clear. There seems to be a main leader with some structures pointing out to the side which distort the temporal stepping behaviour.

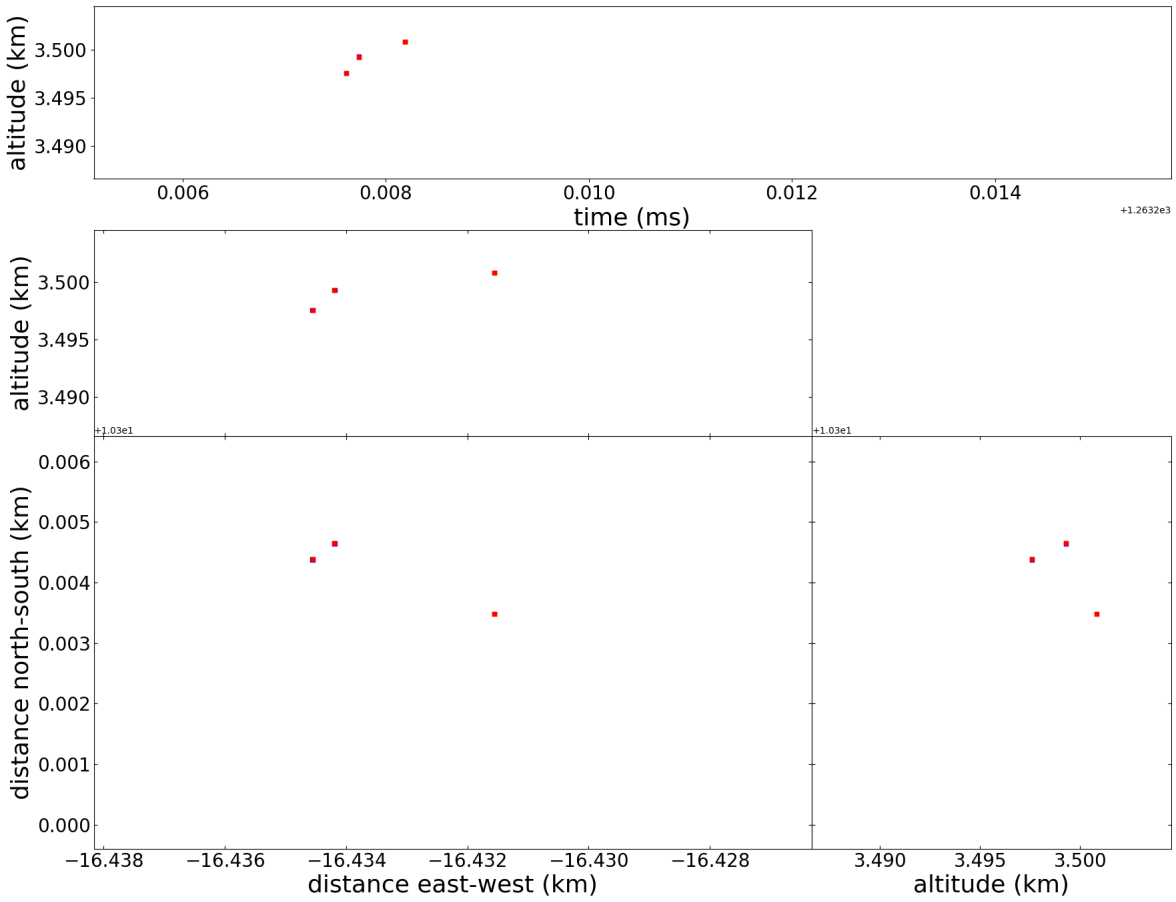

Figure 9.15: A zoom in on the second burst from the left in figure 9.14.

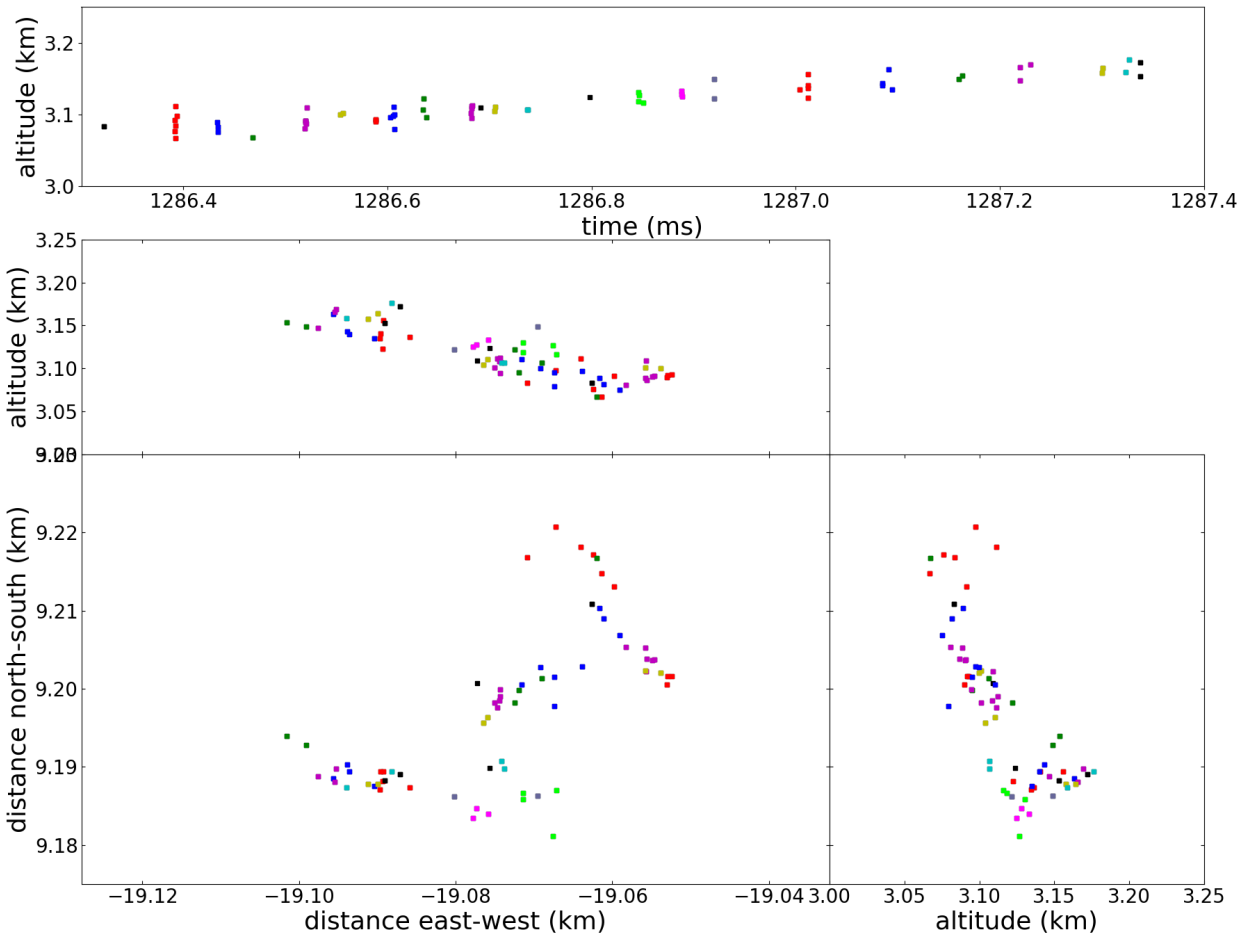

Figure 9.16: This is the same leader as discussed in the results section. This figure shows the total propagation of this leader in space, instead of separate sections of it. In figure 9.18, 9.19, 9.20, and 9.21 some of the bursts are imaged.

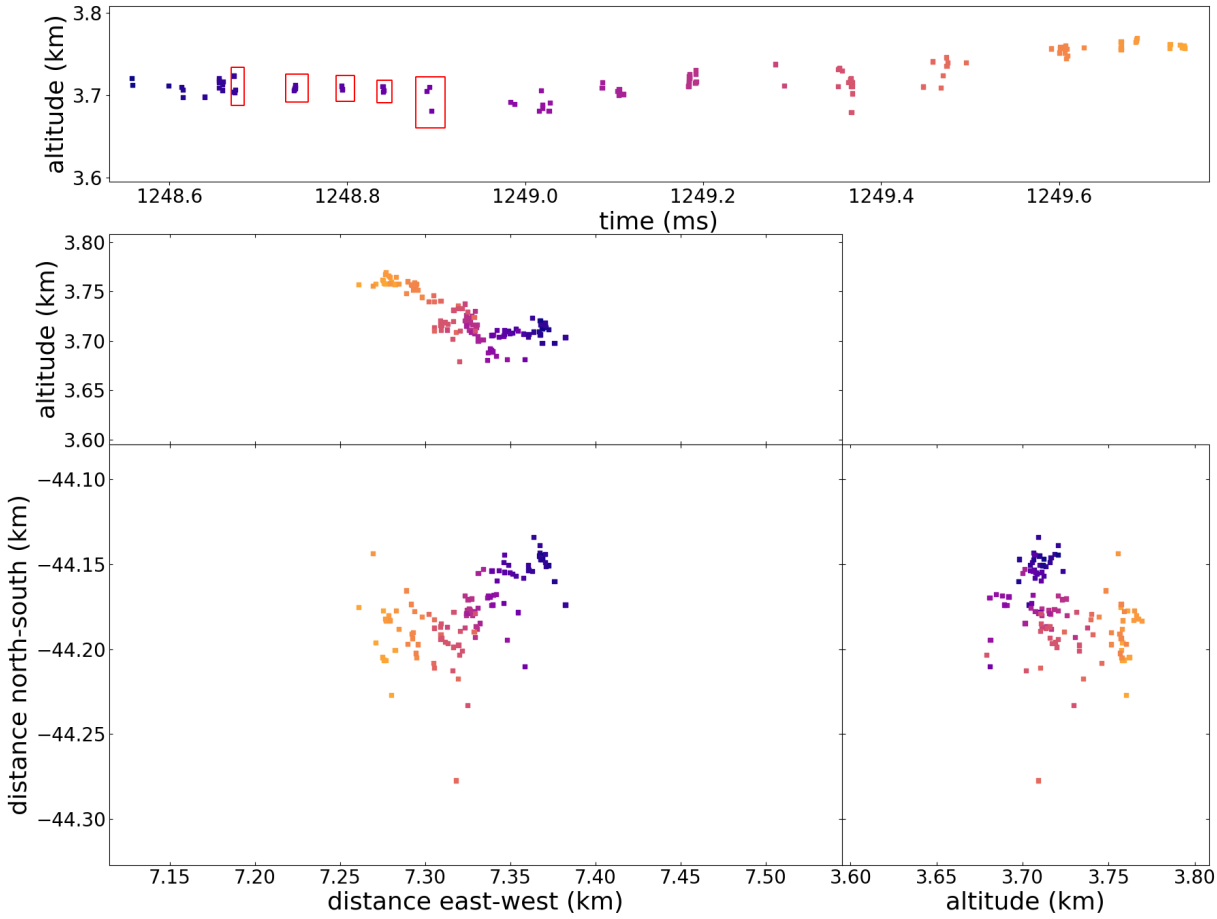

Figure 9.17: Once more the image of the leader treated in the results, the red boxes indicate which bursts are zoomed in on in figure 9.18, 9.19, 9.20, and 9.21.

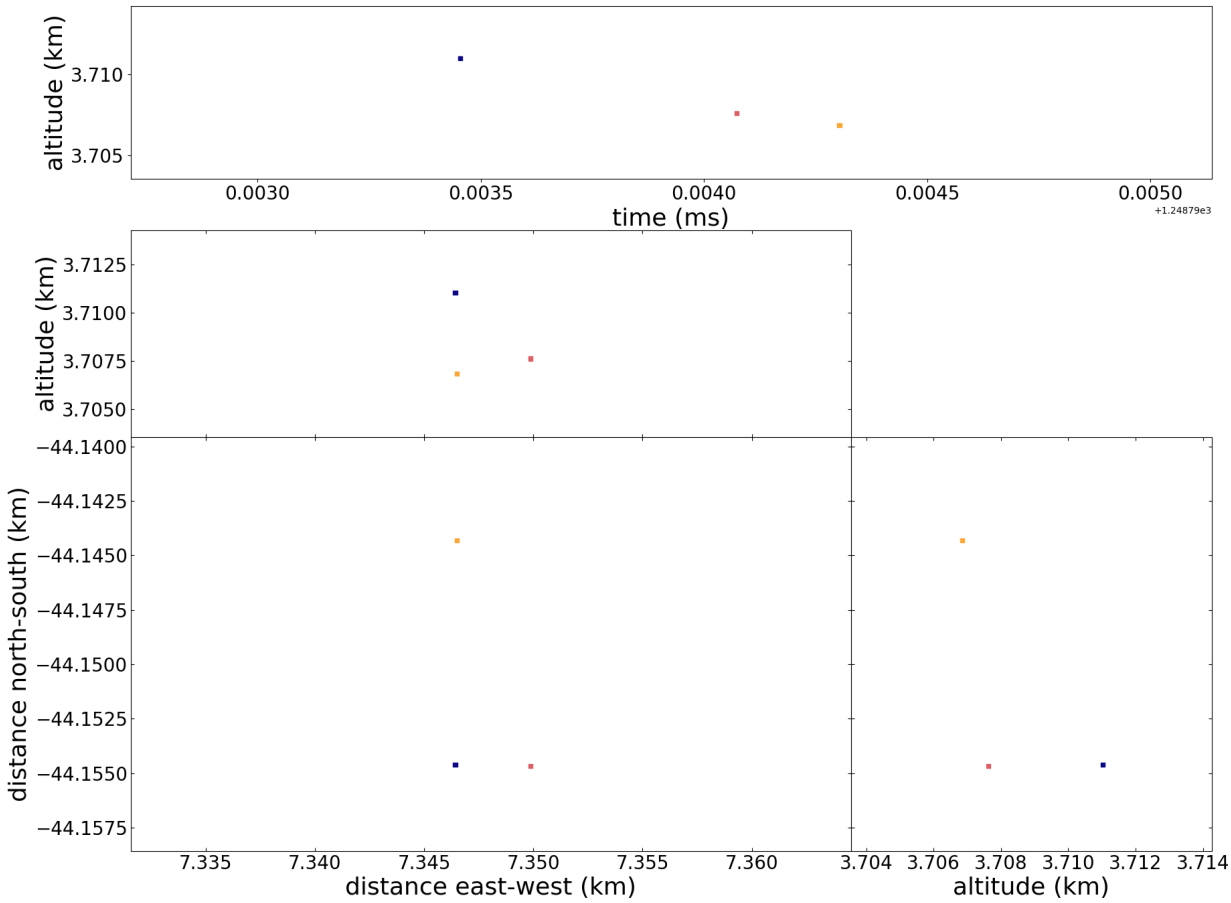

Figure 9.18: Zoom in on one of the bursts of the leader treated in the results section.

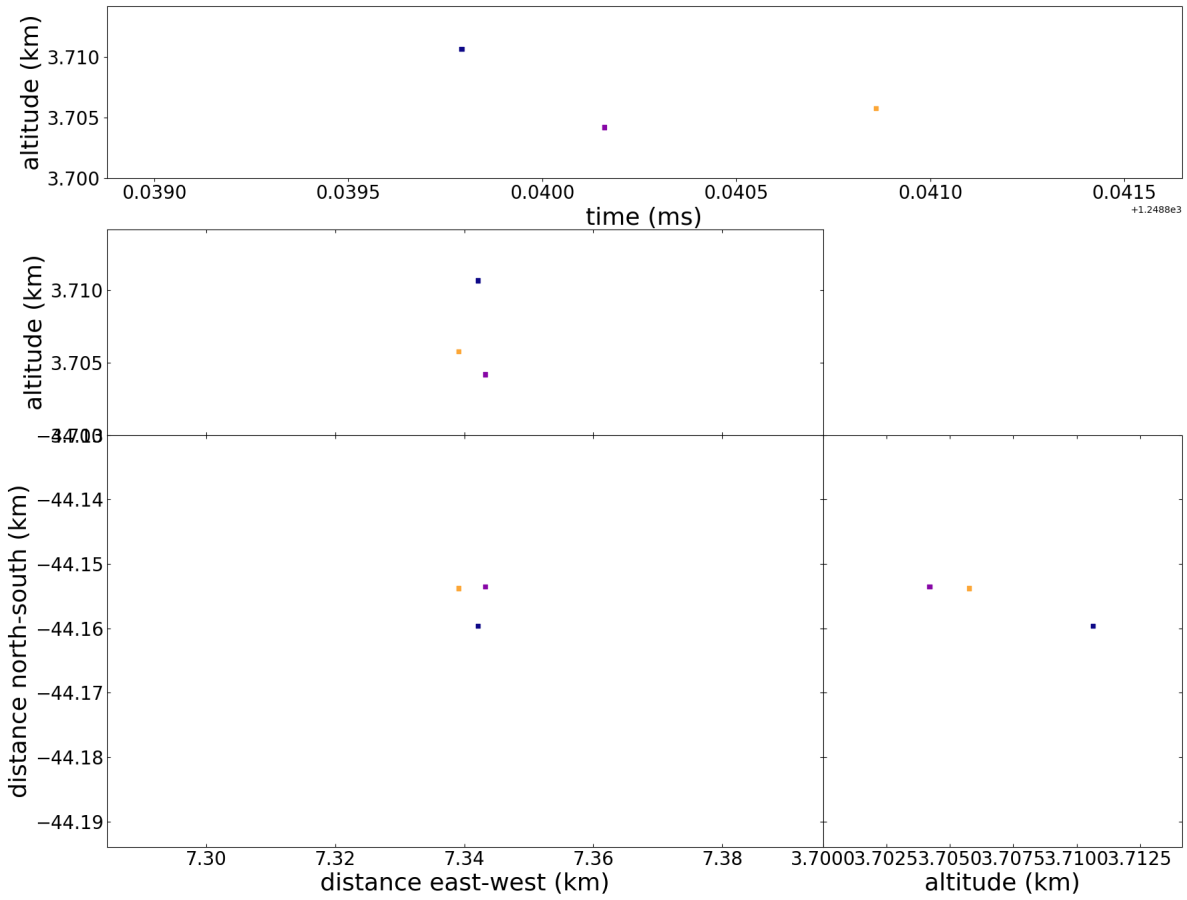

Figure 9.19: Zoom in on one of the bursts of the leader treated in the results section.

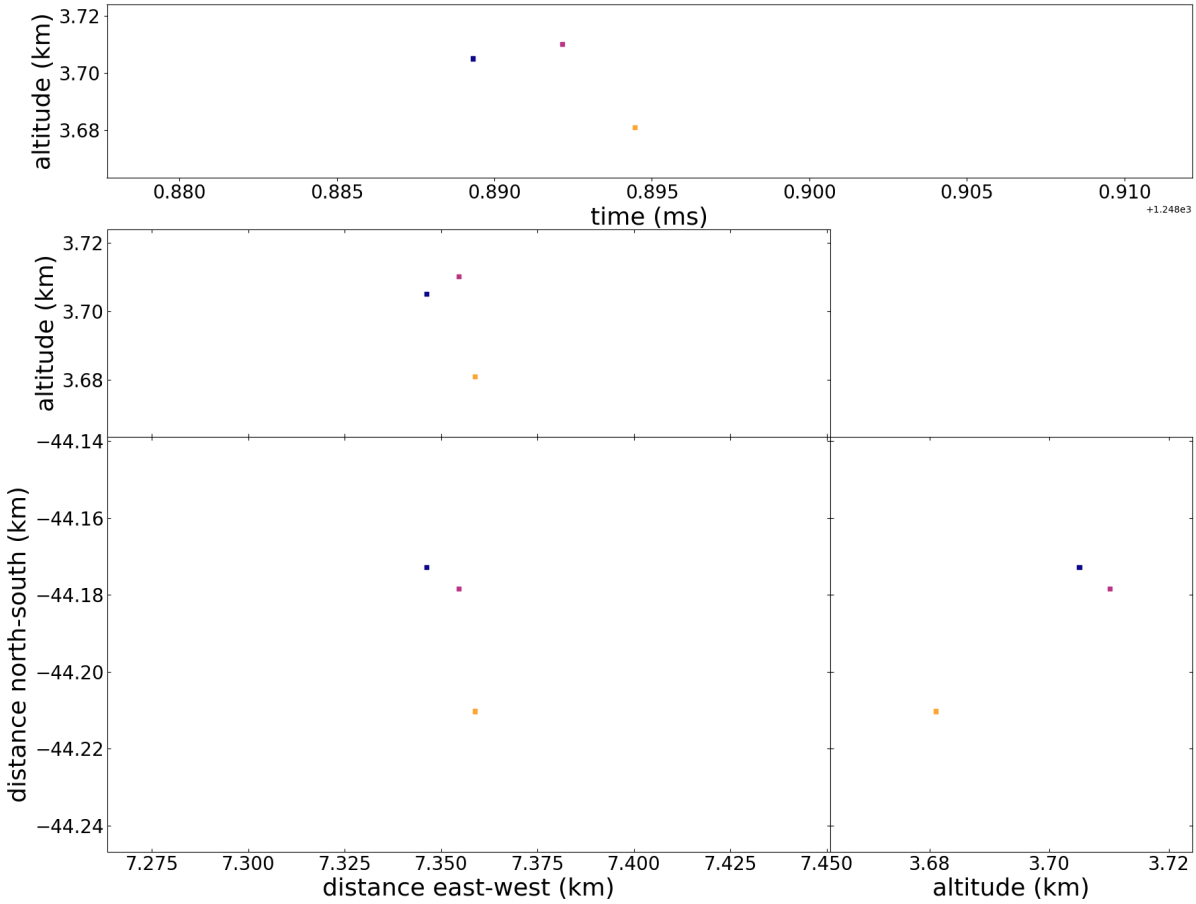

Figure 9.20: Zoom in on one of the bursts of the leader treated in the results section.

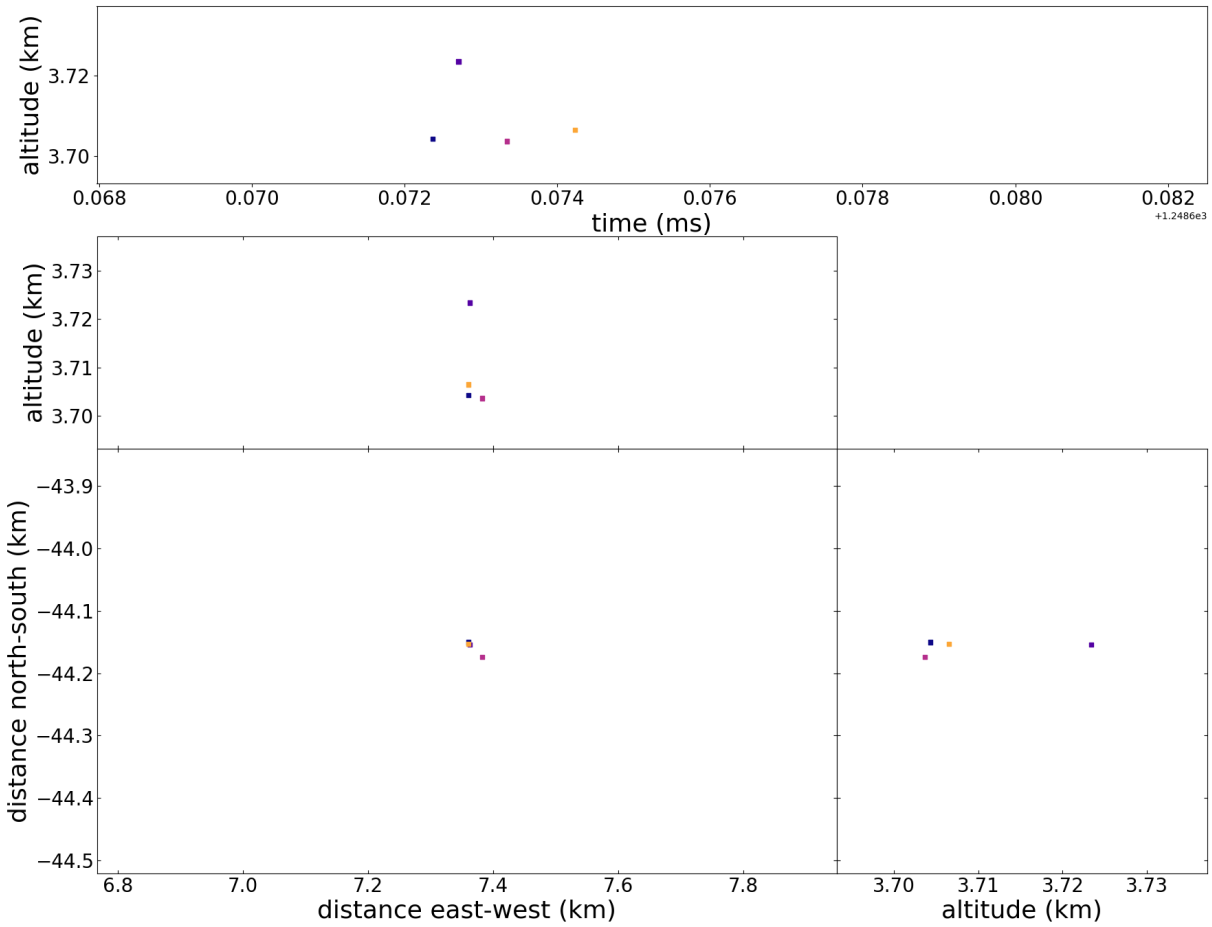

Figure 9.21: Zoom in on one of the bursts of the leader treated in the results section.

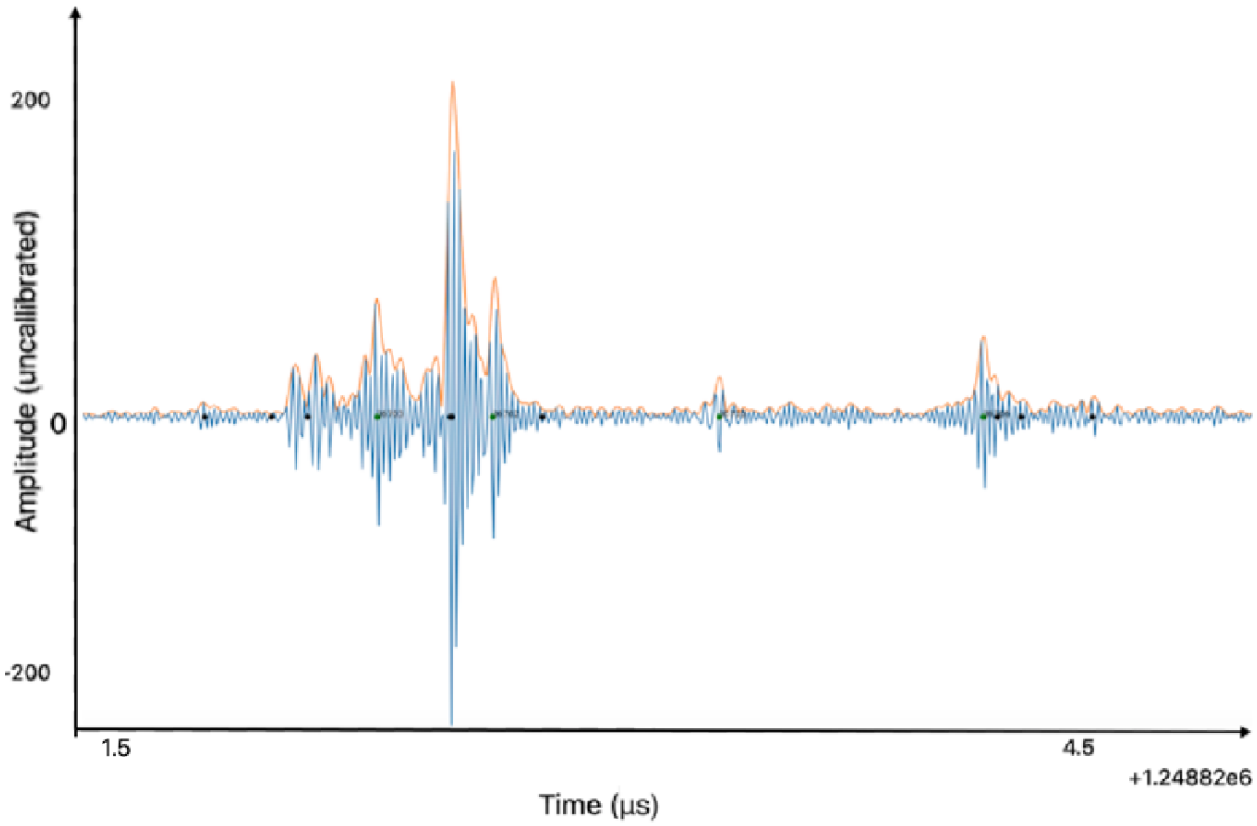

Figure 9.22: Raw data of a burst. Showing the height and width of individual pulses.